Journal of Virology

Antimicrobial Chemotherapy | Full-Length Text

V3 tip determinants of susceptibility to inhibition by CD4-mimetic compounds in natural clade A human immunodeficiency virus (HIV-1) envelope glycoproteins

Saumya Anang,[1,2] Shijian Zhang,[1,2] Christopher Fritschi,[3] Ta-Jung Chiu,[3] Derek Yang,[3] Amos B. Smith III,[3] Navid Madani,[1,2] Joseph Sodroski[1,2]

AUTHOR AFFILIATIONS See affiliation list on p. 15.

ABSTRACT CD4-mimetic compounds (CD4mcs) bind the human immunodeficiency virus (HIV-1) gp120 exterior envelope glycoprotein (Env) and compete for binding to CD4, the host receptor. CD4mcs prematurely trigger conformational changes in Env similar to those induced by CD4, leading to transient activation of infectivity followed by irreversible virus inactivation. Natural HIV-1 variants exhibit a wide range of susceptibilities to CD4mc inhibition, only a small fraction of which can be explained by variation in the gp120 Phe-43 cavity/vestibule where CD4mcs bind. Here, we study Envs from the resistant HIV-1_{BG505} and the more sensitive HIV-1_{191955_A4} clade A strains. The major determinant of the relative sensitivity of the HIV-1_{191955_A4} Env to CD4mcs mapped to a single residue change (F317Y) in the tip of the gp120 V3 variable loop. In the Envs of several HIV-1 strains, replacement of the more prevalent Phe 317 with a tyrosine residue increased virus sensitivity to multiple CD4mcs. Tryptophan substitutions at residues 317 and 316 resulted in increases and decreases, respectively, in sensitivity to CD4mcs. Some of the gp120 V3 changes increased virus sensitivity to inactivation by both CD4mc and cold exposure, phenotypes indicative of increased Env triggerability. Infection of CD4-negative cells expressing the CCR5 coreceptor by these Env variants was triggered more efficiently by CD4mcs. For the panel of studied HIV-1 Envs, resistance to the CD4mcs was associated with decreased ability to support virus entry. These studies illustrate how variation in gp120 outside the CD4mc binding site can influence the sensitivity of natural HIV-1 strains to inhibition by these compounds.

IMPORTANCE CD4-mimetic compounds (CD4mcs) are small-molecule inhibitors of human immunodeficiency virus (HIV-1) entry into host cells. CD4mcs target a pocket on the viral envelope glycoprotein (Env) spike that is used for binding to the receptor, CD4, and is highly conserved among HIV-1 strains. Nonetheless, naturally occurring HIV-1 strains exhibit a wide range of sensitivities to CD4mcs. Our study identifies changes distant from the binding pocket that can influence the susceptibility of natural HIV-1 strains to the antiviral effects of multiple CD4mcs. We relate the antiviral potency of the CD4mc against this panel of HIV-1 variants to the ability of the CD4mc to activate entry-related changes in Env conformation prematurely. These findings will guide efforts to improve the potency and breadth of CD4mcs against natural HIV-1 variants.

KEYWORDS virus, envelope, entry inhibitor, Env, CD4-mimetic compound, resistance, gp120, variable region, V3 loop, strain variation

The binding of the human immunodeficiency virus (HIV-1) envelope glycoprotein (Env) to host cell receptors, CD4 and CCR5/CXCR4, triggers virus entry into the cell (1–11). The Env trimer consists of three gp120 exterior Envs and three gp41

Editor Frank Kirchhoff, Ulm University Medical Center, Ulm, Germany

Address correspondence to Joseph Sodroski, joseph_sodroski@dfci.harvard.edu.

The authors declare no conflict of interest.

See the funding table on p. 16.

Received 28 July 2023
Accepted 12 October 2023

Published 27 October 2023

transmembrane Envs. Prior to receptor engagement, the HIV-1 Env trimer on virions mainly exists in a pretriggered "closed" conformation (State 1) but also samples more "open" conformations (States 2 and 3) (12–15). CD4 binding drives Env from State 1 to State 2 and then into State 3, the prehairpin intermediate (12–18). In the prehairpin intermediate, the heptad repeat (HR1) region of gp41 forms an exposed coiled coil (16–19). Binding of the State 3 Env to the CCR5 or CXCR4 coreceptor is thought to induce the formation of a highly stable gp41 six-helix bundle, which promotes the fusion of the viral and cell membranes (20–25).

The closed nature of the State-1 conformation, significant strain variability, and heavy glycosylation of the HIV-1 Env trimer contribute to the avoidance of potentially neutralizing antibodies (26–29). Amidst conformational and sequence variation, HIV-1 must conserve the gp120 binding sites for its receptors. The binding site for CD4 on gp120 consists of a conserved surface that is conformationally altered by CD4 binding. CD4 binding creates an internal pocket in gp120 called the Phe-43 cavity that is bounded by highly conserved residues from gp120 and a single phenylalanine residue (Phe-43) from CD4 (30). The ~150 $Å^3$ Phe-43 cavity and the surrounding "vestibule" on the gp120 surface comprise the binding sites for two classes of small-molecule HIV-1 entry inhibitors, the CD4-mimetic compounds (CD4mcs) and conformational blockers like BMS-806 and BMS-529 (temsavir) (30–40).

CD4mcs disrupt HIV-1 entry by binding to gp120 in the Phe-43 cavity, directly competing with CD4 but also prematurely triggering Env (31, 40–42). CD4mcs drive the State-1 Env trimer into downstream conformations (States 2 and 3) that, in proximity to a coreceptor-expressing target cell, can mediate HIV-1 infection (42). These CD4mc-induced Env intermediates are short-lived and, in the absence of a coreceptor-expressing target cell, irreversibly decay into inactive, dead-end conformations (41, 42). At CD4mc concentrations that do not completely inhibit HIV-1 infection, the induction of more open Env conformations sensitizes HIV-1 viruses to neutralization and HIV-1-infected cells to antibody-dependent cellular cytotoxicity by otherwise ineffectual antibodies (43–52).

Early CD4mcs discovered using a gp120-CD4 screen exhibited weak antiviral potency against a limited range of HIV-1 isolates (31, 40). Iterative cycles of design, guided by CD4mc-gp120 structures and empirical testing, led to the development of analogs with improved potency (36–38, 53–56). Progressive increases in CD4mc potency have been accompanied by an increase in the breadth of activity against a wider range of HIV-1 strains (37, 38, 57). BNM-III-170, a well-studied CD4mc analog with an indane scaffold, inhibits approximately 70% of a global panel of multi-clade HIV-1 variants (37). Recently developed CD4mcs based on an indoline scaffold exhibit 10- to 20-fold increases in anti-HIV-1 potency compared with BNM-III-170 (57). With the exception of CRF01_AE recombinant HIV-1 (see below), indoline CD4mcs inhibit the entry of every HIV-1 strain tested (57).

Despite significant improvements in the potency and coverage of the lead indoline CD4mcs, primary HIV-1 strains exhibit a 1,000-fold range of sensitivities to their antiviral effect (57). The rank order of sensitivities of lentivirus vectors pseudotyped by diverse HIV-1 Envs is highly correlated among different CD4mcs, suggesting that an intrinsic property of Env determines CD4mc susceptibility (57). With respect to HIV-1 phylogeny, only the CRF01_AE recombinants, in which the imidazole ring of His 375 occupies the Phe-43 cavity, are resistant to the CD4mcs (58–60). In the other phylogenetic clades, HIV-1 strains exhibit the entire range of sensitivities to the CD4mc (57). The susceptibility of most primary HIV-1 strains to CD4mcs is not obviously explained by local variation in the known binding site of these compounds (36–38, 57, 59–61). For example, the Phe-43 cavity of 96% of these HIV-1 strains is bounded by Ser or Thr 375 residues that are compatible with efficient CD4mc binding (58–61).

Pathways to CD4mc resistance preferred by HIV-1 in the absence of immune selection have been studied by passaging HIV-1 in the presence of BNM-III-170 (62). In addition to two changes near the gp120 Phe-43 cavity, a third change in the gp120 inner

domain outside the BNM-III-170 binding site contributed to resistance. Studies with closely matched Env mutants have provided insight into one mechanism whereby Env changes distant from the CD4mc binding site can influence virus sensitivity to these compounds (26, 63–66). To bind and inhibit HIV-1, CD4mcs must induce transitions from State 1 to downstream conformations (26, 31, 35–37, 41, 42, 46, 47, 53–55, 67). Viruses with Envs that have more stable State-1 conformations and, therefore, are less prone to make transitions from State 1 exhibit greater resistance to CD4mcs (26, 63–66). Thus, Env "triggerability" or intrinsic reactivity, a property that is inversely related to the height of the activation barrier separating State 1 and State 2 (13, 26, 27), can significantly affect the susceptibility of HIV-1 Env mutants to inhibition by CD4mcs.

Little is known about the basis for the 1,000-fold range of sensitivities of natural non-CRF01_AE HIV-1 strains to the lead indane and indoline CD4mcs. CD4mcs make backbone contacts or interact with the side chains of highly conserved gp120 residues (37, 55, 57). Thus, an alternative explanation of primary HIV-1 susceptibility involving differences in Env triggerability, which need not be specified by changes near the CD4mc binding site, is appealing. Here, we investigate the basis for the different sensitivity of two clade A primary viruses, HIV-1_{191955_A4} and HIV-1_{BG505}, to BNM-III-170 and potent lead indoline CD4mcs. We map the Env determinant of this difference in CD4mc sensitivity to a single amino acid residue (Tyr/Phe 317) in the tip of the gp120 V3 loop. We explore the effect of changes in this and adjacent V3 residues on the sensitivity of viruses to CD4mcs and cold exposure, two phenotypes known to be influenced by alterations in Env triggerability (63–66, 68). We evaluate the impact of Env resistance to CD4mcs on the ability to mediate infection of cells expressing CD4 and CCR5. We also examine the ability of the Env variants to be activated by CD4mcs to mediate virus infection of CD4-negative, CCR5-expressing cells. These results provide insights into mechanisms whereby Env changes outside the CD4mc binding site can influence the sensitivity of natural HIV-1 strains to inhibition by this class of entry inhibitors.

RESULTS

Determinants of the different sensitivities of the 191955_A4 and BG505 Envs to CD4mcs

HIV-1_{191955_A4}, hereafter referred to as HIV-1_{A4}, and HIV-1_{BG505} are primary clade A viruses (69–71) that exhibit differences in sensitivity to several CD4mcs (Fig. 1A). Compared with HIV-1_{BG505}, HIV-1_{A4} is relatively sensitive to the indane CD4mc BNM-III-170 (37) and to the indoline CD4mcs, CJF-III-192 and CJF-III-288 (57). As expected (57), the indoline CD4mcs inhibited both HIV-1_{A4} and HIV-1_{BG505} more potently than BNM-III-170. As there are more than 120 amino acid residue differences between the A4 and BG505 Env ectodomains, we first attempted to localize the determinants of CD4mc sensitivity to the gp120 or gp41 subunit. The $gp120_Bgp41_A$ chimera, which comprises the BG505 gp120 and A4 gp41, exhibited a level of resistance to the CD4mcs at least as great as that of the BG505 parent virus (Fig. 1A). Conversely, the $gp120_Agp41_B$ chimera was as sensitive to inhibition by the CD4mcs as the A4 parent virus. These results indicate that the main determinants of the differences in CD4mc susceptibility between the A4 and BG505 viruses are located in the gp120 subunit.

The testing of additional A4-BG505 chimeras involving different regions of gp120 allowed us to narrow the number of potential candidates for the CD4mc susceptibility determinants further. The results with one such chimeric Env, $B(V1/V2+gp41)_A$, indicated that the V1/V2 region of BG505 gp120 does not determine the resistant phenotype (Fig. 1A). By contrast, the results with the $B(V3+gp41)_A$ chimera clearly indicate that the BG505 gp120 V3 region is required for the relative resistance of the BG505 Env to the CD4mcs (Fig. 1A). The Env chimeras, $A(N\text{-}gp120)_B$ and $A(C\text{-}gp120)_B$, which share BG505 Env sequences only in the gp120 V3 region, were both resistant to the CD4mcs (Fig. 1A). The CD4mc sensitivity of the $B(V3+gp41)_A$ virus and the CD4mc resistance of the $A(N\text{-}gp120)_B$ and $A(C\text{-}gp120)_B$ viruses exceeded those of the A4 and BG505 parental viruses from which the respective V3 sequences were derived. These results implicate

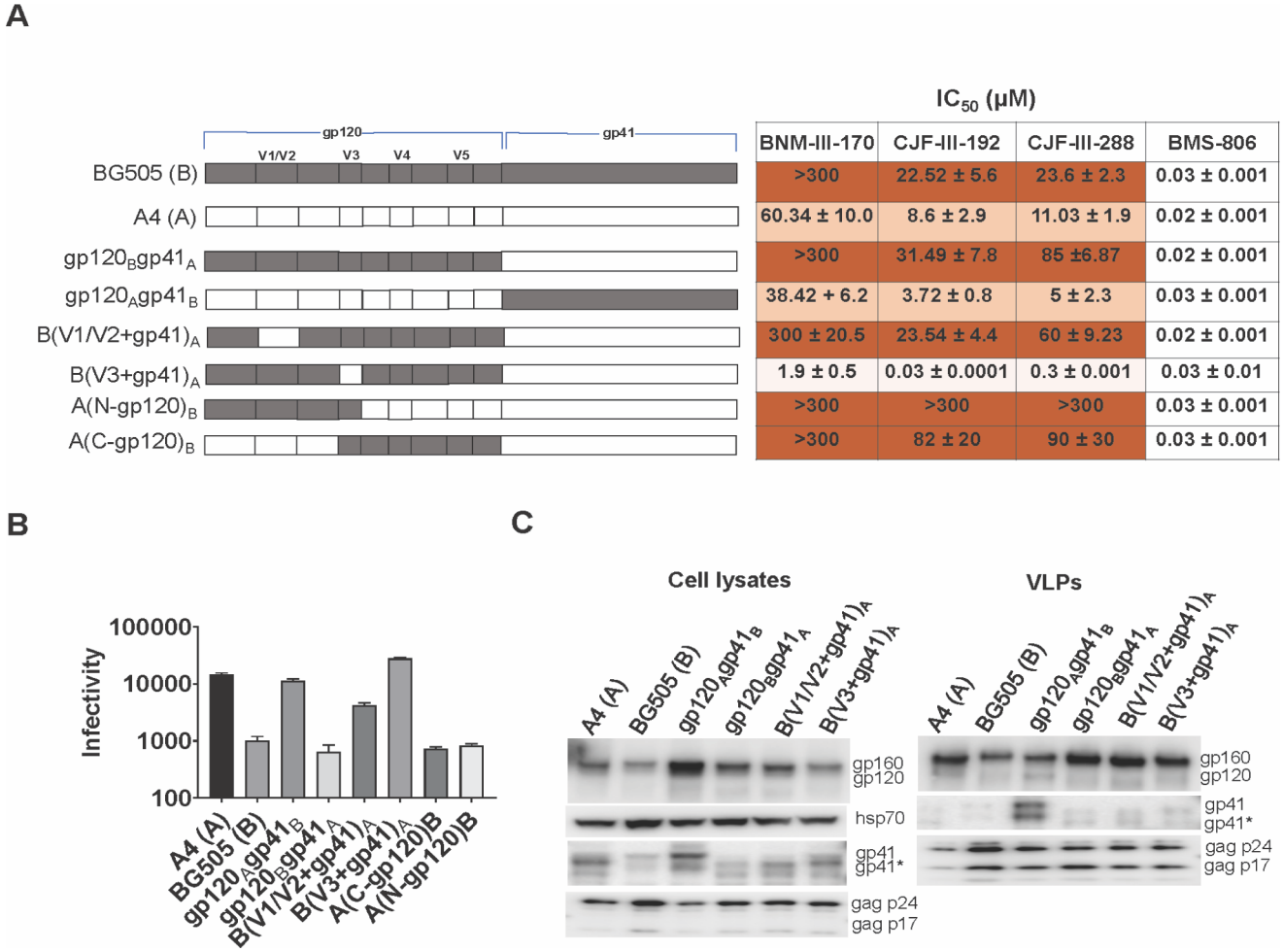

FIG 1 Determinants of the different sensitivities of the BG505 and 191955_A4 Envs to CD4mcs. (A) A schematic representation is shown of the gp120 and gp41 subunits of the BG505 and 191955_A4 (designated A4) Envs and chimeras. The gp120 V1/V2, V3, V4, and V5 variable regions are designated. HEK 293T cells were transfected with plasmids encoding the indicated Envs, HIV-1 packaging proteins, and a luciferase-expressing HIV-1 vector. Pseudoviruses were incubated with different concentrations of the inhibitors for 1 hour at 37°C and then added to Cf2Th-CD4/CCR5 cells. After 2 days of culture, the cells were lysed, the luciferase activity was measured, and the IC_{50} was calculated. The IC_{50} values for inhibition of viruses pseudotyped with the indicated Envs by BNM-III-170, CJF-III-192, CJF-III-288, and BMS-806 are reported as means and standard deviations derived from at least three independent experiments. The intensity of shading is proportionate to the level of CD4mc resistance. (B) The infectivity of viruses with the indicated Envs was measured on Cf2Th-CD4/CCR5 cells. Recombinant luciferase-expressing viruses pseudotyped with the indicated Envs were produced as described above. Forty-eight hours later, cell supernatants containing the pseudotyped viruses were cleared and added in equal volumes to Cf2Th-CD4/CCR5 cells. Two days later, the cells were lysed, and the luciferase activity was measured. Means and standard deviations from at least two independent experiments are reported. (C) The expression level, processing, and virion incorporation of the A4 and BG505 Envs and indicated chimeras are shown. HEK 293T cells were transfected with the packaging plasmids and constructs expressing the Env variants. Cell lysates and virus-like particles (VLPs) were harvested 48 hours later, and equivalent volumes were processed and analyzed by Western blotting for the indicated proteins. A minor form of gp41 resulting from cleavage of the cytoplasmic tail is designated by an asterisk. The results shown are representative of those obtained in three or more independent experiments. However, the relatively high level of gp41 in the VLPs containing the $gp120_Agp41_B$ chimera was not reproduced in other experiments.

the gp120 V3 region in determining sensitivity to the CD4mcs and suggest that other gp120 sequences can influence the degree of the observed phenotypes. The parental A4 and BG505 viruses and the viruses with chimeric Envs were comparably inhibited by the conformational blocker, BMS-806 (Fig. 1A). Thus, even though CD4mcs and BMS-806 bind to similar gp120 regions (30–40), sensitivity to these entry inhibitors differs among these Env variants.

The A4-BG505 chimeric Envs exhibited different levels of efficiency with which they supported virus infection of $CD4^+CCR5^+$ cells (Fig. 1B). These differences were not related to variation in the level of Env expression or incorporation into virus particles (Fig. 1C). The relationship between CD4mc resistance and infectivity will be explored for these and other Env variants below.

The gp120 V3 loop as a determinant of CD4mc susceptibility

The above results indicate that A4- and BG505-specific sequences in the gp120 V3 region determine the respective sensitivity and resistance of the parental viruses to the CD4mcs. We, therefore, tested whether particular BG505 V3 amino acid residues are essential for maintaining the resistant phenotype. Comparison of the A4 and BG505 gp120 V3 sequences identified six amino acid differences (Fig. 2A). Our attention was drawn to the four differences at residues 307/308 and 317/318, which are symmetrically positioned at the tip of the V3 loop (72). While polymorphisms in three of these V3 residues are common in HIV-1 strains, Tyr 317 in the A4 Env is unusual (59, 60). Approximately 79% of HIV-1 strains have a phenylalanine residue at this position; in the remaining strains, Leu and Trp are common substitutions, Met is less common, and Tyr is only occasionally seen. We evaluated the effect of introducing the F317Y change in the BG505 Env. Viruses with the $B(307+317)_A$ and $B(317)_A$ Envs were more sensitive to the CD4mcs than the BG505 virus, with sensitivities similar to or even greater than those of the A4 virus (Fig. 2A and B). Thus, the Tyr 317 substitution in V3 is sufficient to explain the increased CD4mc sensitivity of the A4 virus relative to that of the BG505 virus.

We evaluated whether the BG505 V3 sequences were sufficient to render the A4 virus resistant to the CD4mcs. The $A(307+308+317+318)_B$, $A(307+317)_B$, and $A(317)_B$ viruses were as resistant to the CD4mcs as the BG505 virus (Fig. 2A and B). The $A(307)_B$ virus exhibited an intermediate level of resistance to the CD4mcs. The expression and ability to support infection of these Envs are shown in Fig. 2C and D. The level of gp120 shedding from the virus particles induced by CJF-III-288 roughly corresponded to the sensitivity of the viruses to inhibition by CJF-III-288 (Fig. 3A through C). Our results suggest that variation in the gp120 V3 tip is both necessary and sufficient to account for the different susceptibilities of the A4 and BG505 viruses to CD4mcs.

Effect of V3 changes on CD4mc sensitivity in other HIV-1 strains

We asked whether the alteration of Phe 317 to the less-common tyrosine residue would alter CD4mc sensitivity in other HIV-1 strains. We introduced the F317Y change into the Envs of $HIV\text{-}1_{191084}$, another clade A virus, and $HIV\text{-}1_{CRF02\_AG253.11}$, a tier-3 clade AG recombinant virus (69, 74–76). In both HIV-1 strains, the F317Y change resulted in increased sensitivity to the CD4mcs (Fig. 4A). Thus, the effect of substitution of a tyrosine residue at Phe 317 on CD4mc sensitivity applies to multiple HIV-1 strains. The expression and ability to support infection of these Envs are shown in Fig. 4B and C. We note that the wild-type AG253.11 Env was less efficient in supporting virus infection than the other Envs studied, despite a comparable level of Env expression and incorporation into virus particles.

Hydrophobic aromatic or aliphatic amino acids are found at residue 317 in most HIV-1 strains (59, 60). We asked if a hydrophobic Trp residue at 317 or the adjacent 316 position would influence HIV-1 susceptibility to inhibition by CD4mcs. The A316W change has been used to decrease the exposure of the V3 loop on soluble gp140 SOSIP.664 trimers (77, 78). Although the BG505 (F317W) virus was inhibited by CD4mcs comparably to the wild-type BG505 virus, the Y317W change in the A4 Env and the F317W change in the AD8 Env rendered the viruses more sensitive to the CD4mcs (Fig. 5A and B). By contrast, viruses with the A316W change were slightly or moderately more resistant to CD4mcs. These results indicate that changes in the tip of the gp120 V3 loop can affect the susceptibility of viruses from multiple HIV-1 strains to inhibition by CD4mcs. The expression and ability to support infection of these Envs are shown in Fig. 5C and D.

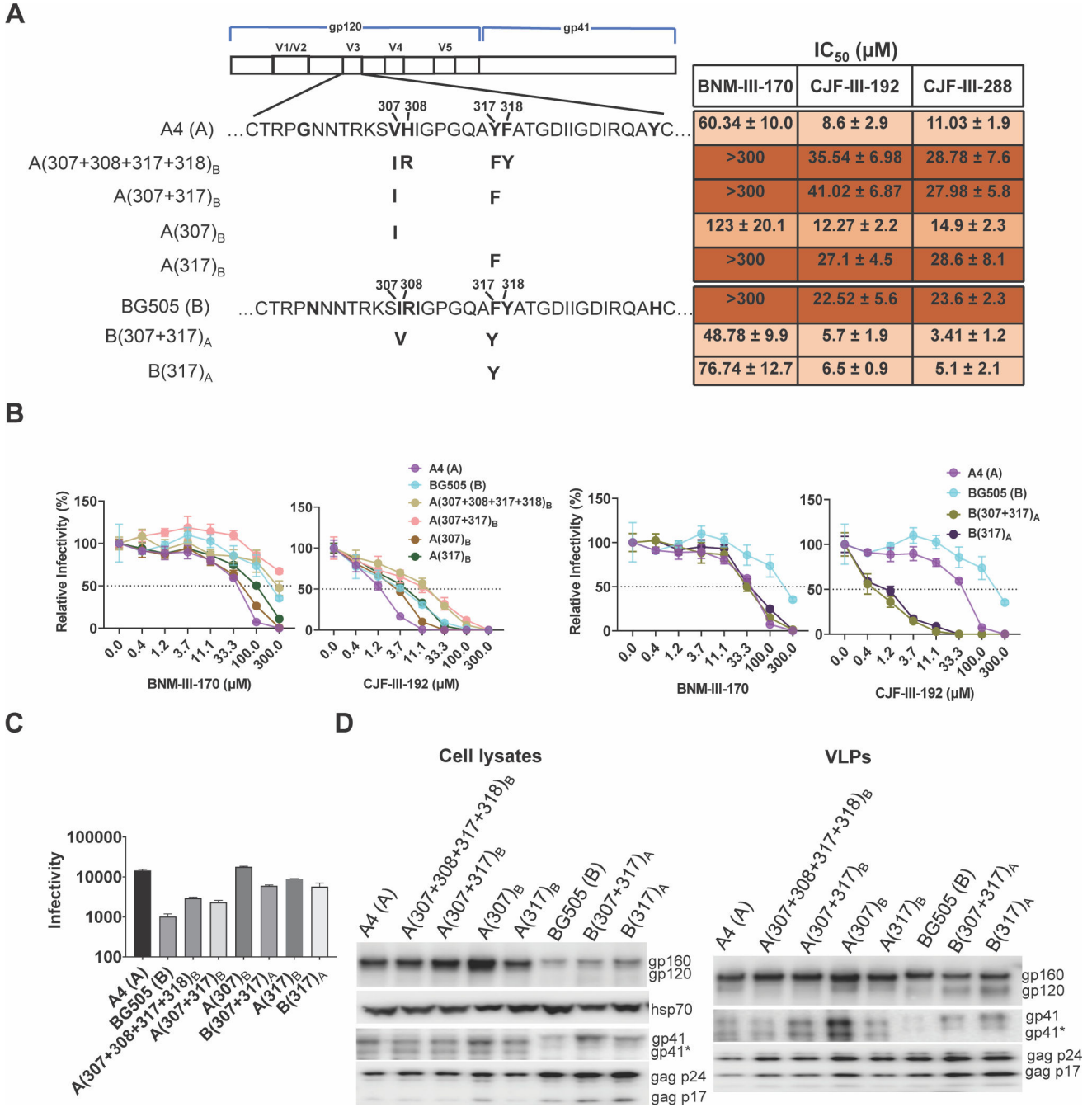

FIG 2 Analysis of the gp120 V3 loop as a determinant of CD4mc susceptibility. (A) The sequences of the A4 and BG505 gp120 V3 loops are aligned beneath the schematic representation of the HIV-1 Env. Amino acid residues that differ between the A4 and BG505 Envs are in bold. The amino acid residues changed in each Env variant are shown in bold beneath the parental Env. Standard HIV-1 Env amino acid numbering is used here and throughout the manuscript (73). The IC_{50} values for inhibition of pseudovirus infection by the CD4mcs were calculated as described in the Fig. 1A legend and are reported as means and standard deviations derived from at least three independent experiments. The intensity of shading is proportionate to the level of CD4mc resistance. (B) The CD4mc dose-inhibition curves for recombinant viruses pseudotyped by the indicated Envs are shown. The relative infectivity represents the level of infection of Cf2Th-CD4/CCR5 target cells observed in the presence of the indicated concentration of CD4mc compared to the level of infection in the absence of the CD4mc. The means and standard deviations derived from triplicate measurements within a typical experiment are reported. (C) The infectivity of viruses with the indicated Envs is shown. The infectivity was measured on Cf2Th-CD4/CCR5 cells as described in the legend to Fig. 1B. Means and standard deviations derived from two independent experiments are reported. (D) The expression level, processing, and virion incorporation of the indicated Envs were evaluated as described in the Fig. 1C legend.

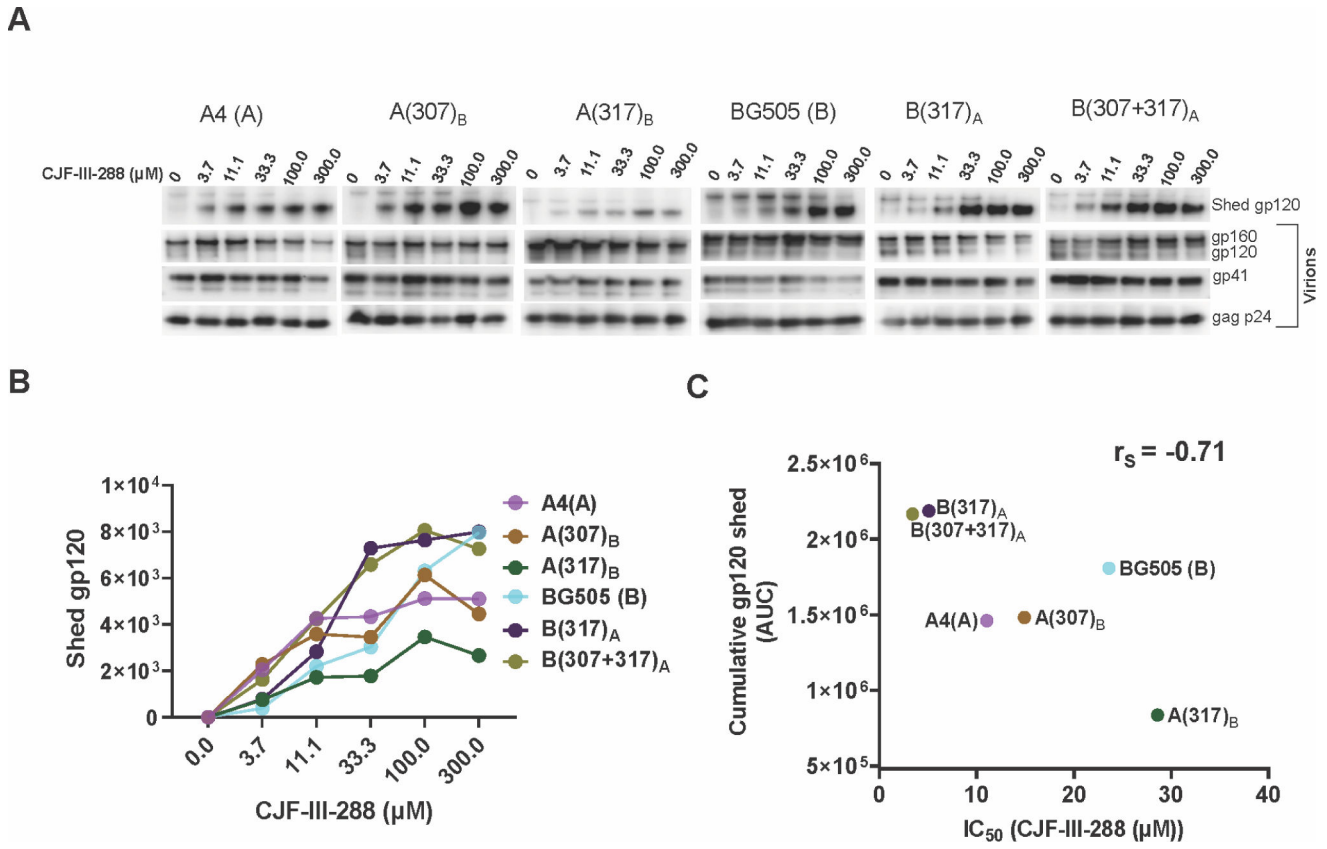

FIG 3 Relationship between susceptibility of HIV-1 Env variants to CD4mc-induced gp120 shedding and virus sensitivity to CD4mc inhibition of infection. (A) CJF-III-288-induced shedding of gp120 from virions with the indicated Envs was measured. Virions were produced transiently from HEK 293T cells transfected with pNL4-3 proviral constructs containing the A4, A(307)$_B$, A(317)$_B$, BG505, B(317)$_A$, and B(307+317)$_A$ *env* genes. Viruses were harvested, clarified by low-speed centrifugation, filtered (0.45 μm), and pelleted at 14,000 × *g* for 1.5 hours at 4°C. The virus pellet was resuspended in 1× phosphate-buffered saline (PBS) and incubated with the indicated concentrations of CJF-III-288 for 2.5 hours at 37°C. The viruses were then pelleted; the virus pellet was lysed, and the supernatant containing shed gp120 was incubated with Galanthus nivalis lectin beads. The viral lysates and the proteins captured on the GNL beads were Western blotted to detect the indicated HIV-1 proteins. (B) For each Env variant, the shed gp120 bands in the Western blot in A were measured and plotted against the concentration of CJF-III-288 incubated with the viruses. (C) The areas under the curves (AUCs) were measured from the plot shown in B. The correlation between the AUCs and the IC_{50} values of CJF-III-288 for inhibition of the corresponding pseudoviruses is shown. r_S = Spearman rank-order correlation coefficient.

CD4 activation of mutant virus infection

CD4mcs induce short lived, activated Env intermediates that irreversibly decay into dead-end conformations (31, 41, 42). To investigate whether V3 loop changes affect this process, we examined the ability of the viruses with wild-type and mutant Envs to infect CD4-negative, CCR5-expressing cells in the presence of increasing concentrations of the CD4mcs. The activating effects of BNM-III-170 and CJF-III-288 were similar (Fig. 6A and B). Compared with the wild-type BG505, AD8, 191084, and AG253.11 viruses, the viruses with Tyr or Trp substitutions at residue 317 were generally activated more efficiently by the CD4mcs. Conversely, the Y317F change in the A(317)$_B$ mutant decreased CD4mc activation relative to that of the wild-type A4 virus. Compared with the wild-type AD8 virus, viruses with the A316W Env were less efficiently activated by CD4mcs.

We evaluated the relationships among the viral phenotypes of the Env variants in this study. The sensitivities of the virus variants to inhibition by BNM-III-170 and CJF-III-288 were highly correlated (Fig. 7A); therefore, we used virus sensitivity to CJF-III-288 inhibition to evaluate potential relationships with other viral phenotypes. For viruses with V3 loop Env variants, there is a strong correlation between sensitivity to CJF-III-288 inhibition and activation by the CD4mcs (Fig. 7B).

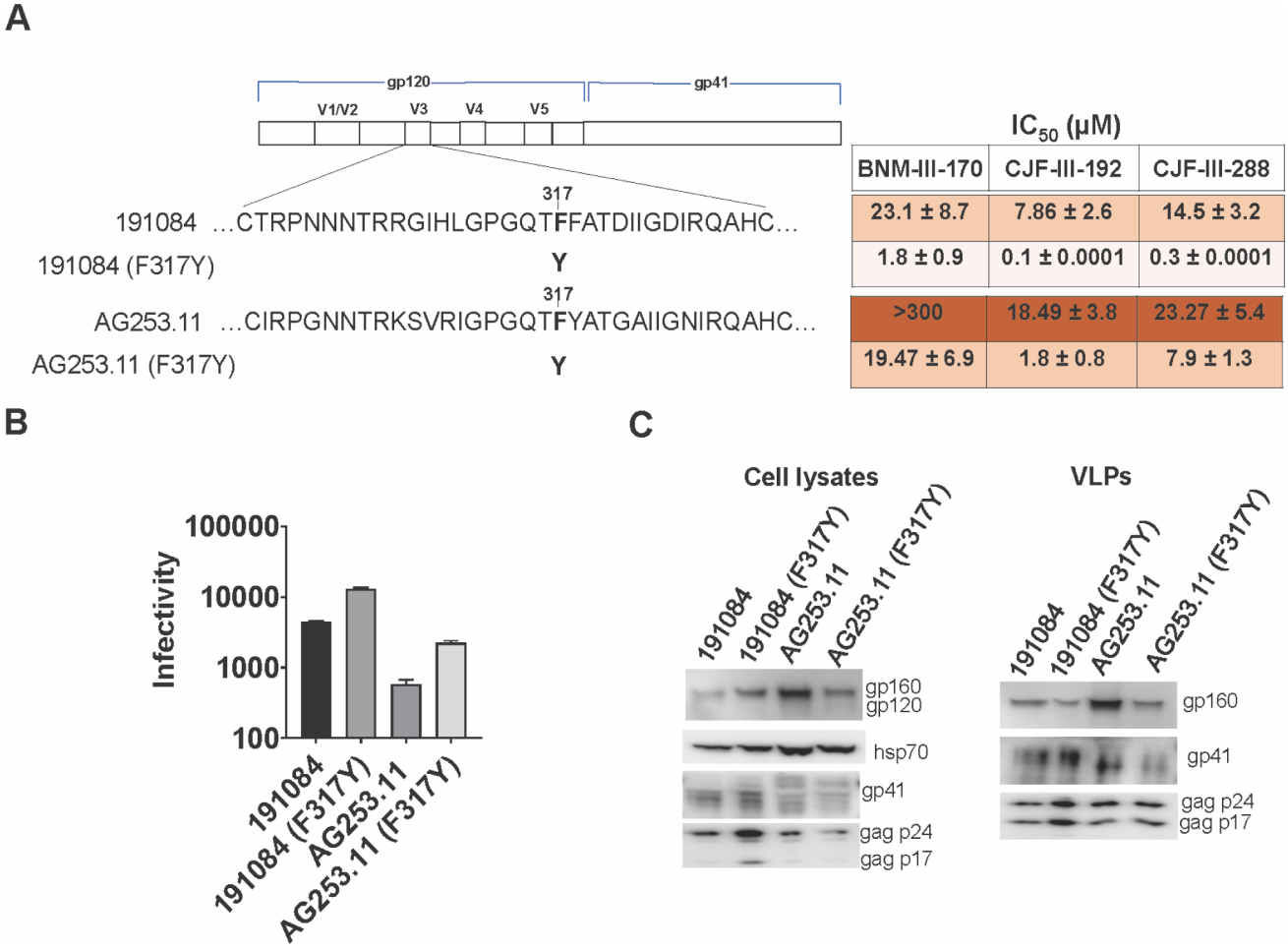

FIG 4 Effect of changes in V3 residue 317 on CD4mc sensitivity in other HIV-1 strains. (A) Sequences of the V3 loops of the 191084 and AG253.11 Envs and F317Y mutants are shown beneath the schematic of the HIV-1 Env. The IC_{50} values for inhibition of infection by the CD4mcs were calculated as described in the Fig. 1A legend and are reported as means and standard deviations derived from at least three independent experiments. The intensity of shading is proportionate to the level of CD4mc resistance. (B) The infectivity of viruses with the indicated Envs is shown. The infectivity was measured on Cf2Th-CD4/CCR5 cells as described in the legend to Fig. 1B. (C) The expression level, processing, and virion incorporation of the indicated Envs were evaluated as described in the legend to Fig. 1C.

Cold sensitivity of mutant viruses

One of the phenotypes associated with alterations in the stability of the State-1 conformation of the HIV-1_{AD8} Env is a change in the sensitivity of the functional viral spike to inactivation by exposure to 0°C (63, 64, 79, 80). We evaluated the infectious half-life following incubation on ice for recombinant viruses pseudotyped by Env variants selected from the studies above. The infectivity of the viruses with the primary HIV-1 Envs exhibited a range of sensitivity to cold (Fig. 6C). Compared with the wild-type A4, AD8, 191084, and AG253.11 viruses, the viruses with Tyr or Trp substitutions at residue 317 were inactivated more rapidly at 0°C. By contrast, the A4 and AD8 viruses with the A316W change were more resistant to cold inactivation. For viruses pseudotyped with this panel of Env variants, there is a good correlation between sensitivity to CJF-III-288 inhibition and cold inactivation (Fig. 7C).

Relationship between virus sensitivity to CD4mcs and infectivity

The relationship between the susceptibility to inhibition by CJF-III-288 and infectivity for the panel of HIV-1 Env variants used in this study is shown in Fig. 7D. Virus infectivity varied inversely with resistance to the CD4mc.

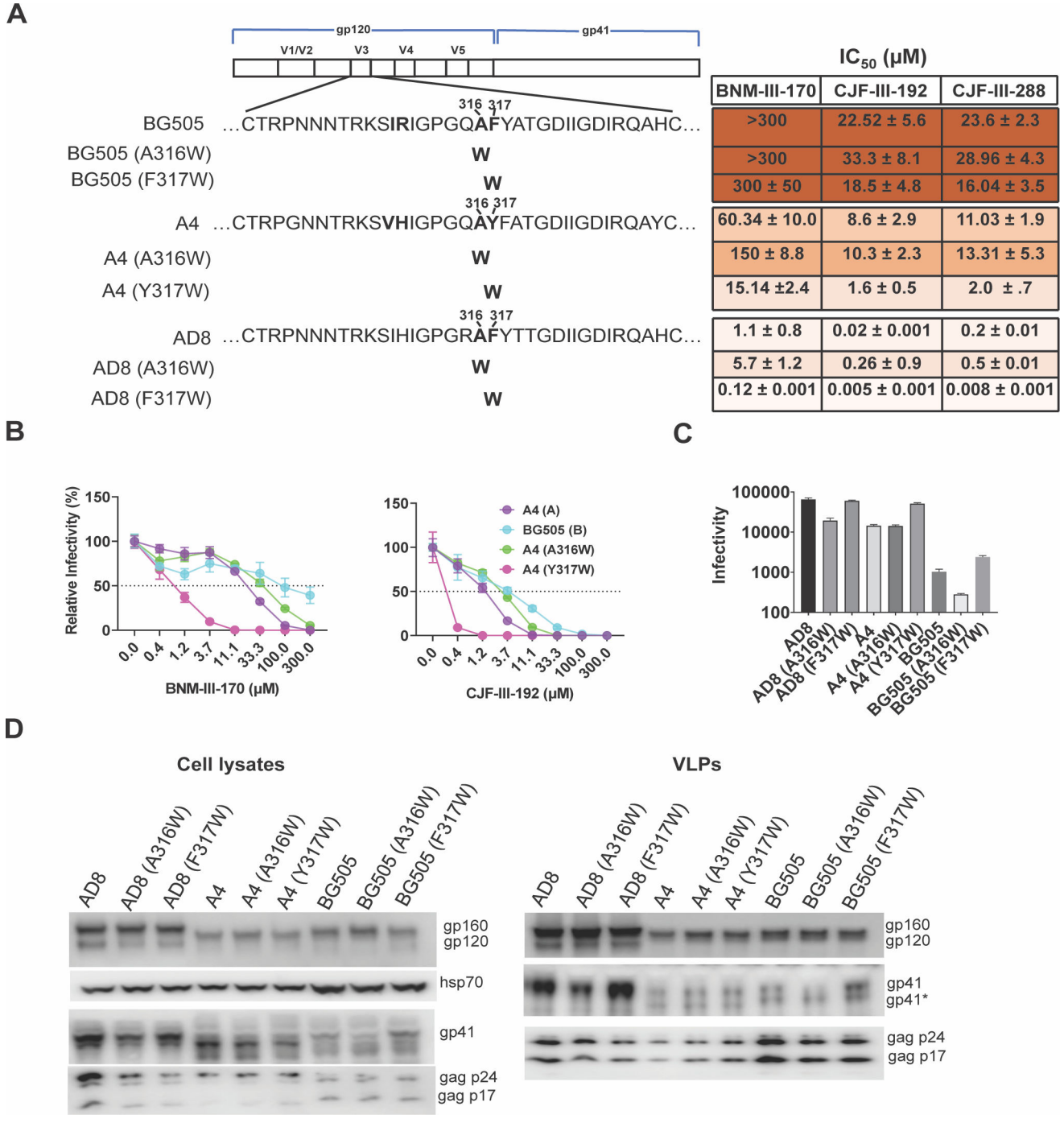

FIG 5 Effect of hydrophobic changes in the gp120 V3 loop. (A) Sequences of the gp120 V3 region of the BG505, A4, and AD8 Envs are shown, along with the hydrophobic Trp substitutions made in the V3 loop mutants, beneath the HIV-1 Env schematic. The IC_{50} values for inhibition of infection by the CD4mcs were calculated as described in the Fig. 1A legend and are reported as means and standard deviations derived from at least three independent experiments. The intensity of shading is proportionate to the level of CD4mc resistance. (B) The CD4mc dose-inhibition curves for recombinant viruses pseudotyped by the indicated Envs are shown. The relative infectivity on Cf2Th-CD4/CCR5 target cells following incubation of the viruses with the indicated concentration of CD4mcs was measured as described in the Fig. 2B legend. The means and standard deviations derived from triplicate measurements within a typical experiment are reported. (C) The infectivity of viruses with the indicated Envs is shown. The infectivity was measured on Cf2Th-CD4/CCR5 cells as described in the legend to Fig. 1B. (D) The expression level, processing, and virion incorporation of the indicated Envs were evaluated as described in the legend to Fig. 1C.

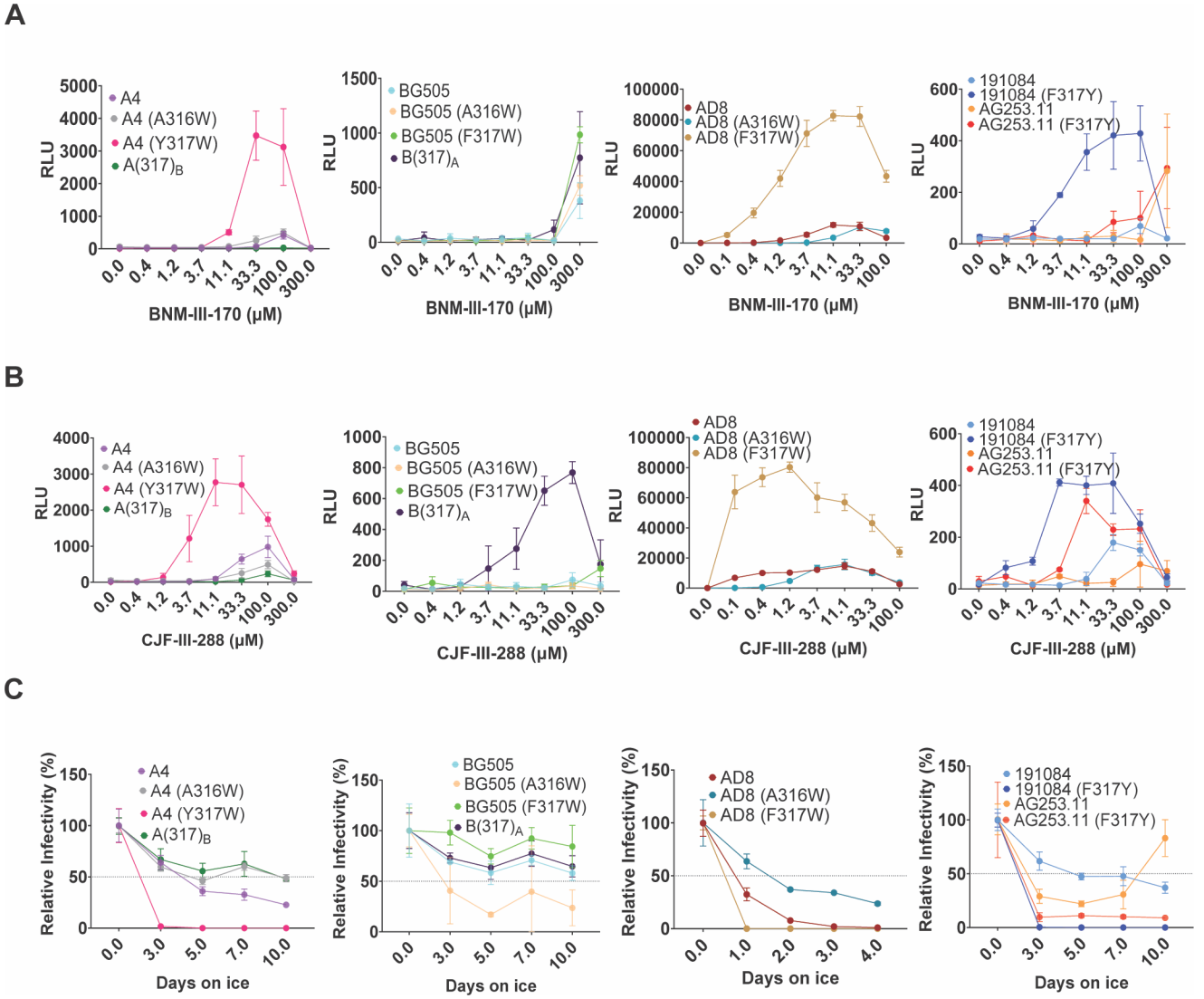

FIG 6 Activation of HIV-1 infection by CD4mcs and sensitivity to cold inactivation. Activation of infection of CD4-negative, CCR5-expressing cells by BNM-III-170 (A) and CJF-III-288 (B) was evaluated for HIV-1 variants with wild-type and mutant A4, BG505, AD8, 191084, and AG253.11 Envs. HEK 293T cells were transfected with plasmids expressing the indicated Envs, HIV-1 packaging proteins, and a luciferase-expressing HIV-1 vector. After 48 hours, pseudoviruses were harvested and incubated with Cf2Th-CCR5 cells in 96-well plates. The plates were centrifuged at 600 × *g* for 30 min at 21°C. Medium containing serial dilutions of BNM-III-170 or CJF-III-288 was then added. After incubation at 37°C in a CO_2 incubator for 48 hours, the cells were lysed, and luciferase activity was measured. RLU, relative light units. (C) To evaluate cold sensitivity, pseudotyped viruses were produced as described in the Fig. 1A legend and were incubated on ice for the indicated times, after which the virus infectivity was measured. In A–C, the means and standard deviations of triplicate measurements are shown. The experiments were repeated with comparable results.

DISCUSSION

Even when the highly resistant CRF01_AE recombinant HIV-1 strains are excluded, primary HIV-1 strains exhibit a 1,000-fold range of IC_{50} values with respect to inhibition by CD4mcs (37, 57). The rank orders of sensitivities of HIV-1 Envs to different CD4mcs are highly correlated, indicating that Env sequences determine virus sensitivity to multiple CD4mcs (57). For the panel of Env variants used in this study, sensitivity to BNM-III-170 and CJF-III-288 correlated. A substantial fraction of the variation in primary HIV-1 sensitivity to CD4mcs is apparently determined by changes in Env elements outside of the known CD4mc binding sites (53–57). Changes in Env triggerability, which is governed by the activation energy barrier between State 1 and downstream Env conformations,

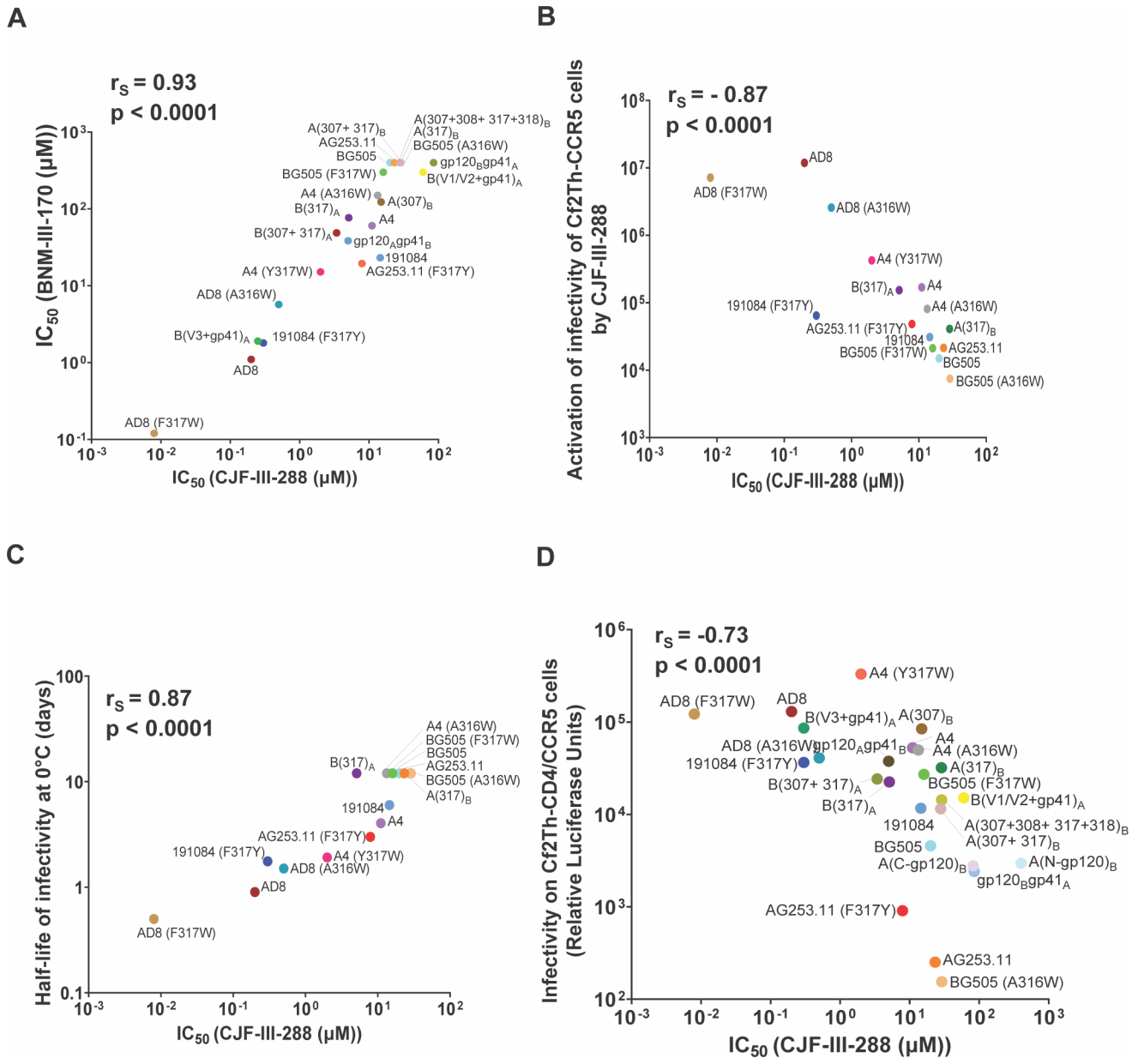

FIG 7 Correlations between viral phenotypes associated with Env variants. (A) The correlation between the CJF-III-288 and BNM-III-170 IC_{50} values (in micromolar) for inhibition of pseudovirus infection of Cf2Th-CD4/CCR5 cells is shown for the Env mutants in this study. (B) The relationship between inhibition of infection of Cf2Th-CD4/CCR5 cells (on the x-axis) and activation of infection of Cf2Th-CCR5 cells (on the y axis) by CJF-III-288 is shown for the indicated pseudovirus variants. The x-axis values represent the IC_{50}'s for each Env from Fig. 1A, 2A, 4A, and 5A. The y-axis values represent the areas under the curve calculated from the activation graphs in Fig. 6B. (C) The relationship between inhibition of infection of Cf2Th-CD4/CCR5 cells (on the x-axis) by CJF-III-288 and sensitivity to cold exhibited by viruses pseudotyped with different Envs is shown. The x-axis values are as in B. The y-axis values represent the half-life of infectivity at 0°C obtained from the experiments shown in Fig. 6C. (D) The relationship between inhibition of infection of Cf2Th-CD4/CCR5 cells (on the x-axis) by CJF-III-288 and infectivity of viruses with the different Envs is shown. The x-axis values are as in B. The y-axis values represent the viral infectivities from Fig. 1B, 2C, 4B, and 5C. The Spearman rank-order correlation coefficients (r_S) and two-tailed p values are shown for each of the graphs.

correlate with CD4mc sensitivity for carefully matched panels of HIV-1_{AD8} Env mutants (64). Additional studies are needed to evaluate the hypothesis that alterations in Env triggerability contribute to the variation in the sensitivity of natural HIV-1 strains to CD4mcs.

The difference in sensitivity of the A4 and BG505 Envs to CD4mcs was determined by the Phe/Tyr 317 polymorphism in the tip of the gp120 V3 loop. The tyrosine residue in

the A4 Env is infrequent at this position and is less hydrophobic than the more common Phe, Leu, or Trp residues. In available Env structures, the V3 loop projects toward the trimer axis at the membrane-distal apex (80–83) (Fig. 8A). Hydrophobic packing in the trimer apex has been suggested to contribute to the maintenance of the closed, pretriggered Env conformation (13, 29, 84). Based on this model, the more polar tyrosine 317 residue may disrupt packing of the trimer apex and predispose the pretriggered Env to open into downstream conformations. The phenotypes of the A316W and A317W mutants demonstrate that hydrophobic substitutions in this region may result in either increases or decreases in CD4mc resistance, respectively. If hydrophobic packing of the V3 tip is important for maintenance of a pretriggered state, the large tryptophan indole ring may be better accommodated at position 316 rather than 317. Trp 316 has been suggested to stabilize sgp140 SOSIP.664 Env trimers by stacking against Tyr 318 (78). In any case, Phe/Tyr 317 is located approximately 14 Angstroms from the nearest gp120 residue that contacts the CD4mcs, and thus, these V3 polymorphisms exert their phenotypic effects over a distance (Fig. 8B).

Our results reveal the functional consequences of naturally occurring polymorphisms in residue 317. In addition to conferring an increase in sensitivity to CD4mcs, Tyr 317 increased CD4mc-induced gp120 shedding and activation of infection of CD4-negative, CCR5-expressing cells. For the entire panel of Env mutants evaluated, virus sensitivity to CJF-III-288 inhibition correlated with CD4mc activation of infection, virus infectivity, and cold sensitivity. The latter two Env phenotypes are evaluated in the absence of CD4mcs and, therefore, provide independent indicators of increased Env triggerability (26, 63, 64, 79). An increase in triggerability specified by V3 residue 317 apparently contributes to the moderate increase in replicative ability and cold sensitivity of the A4 virus compared with the BG505 virus. The development of resistance to CD4mcs through down-modulation of Env triggerability is expected to incur a fitness cost, consistent with the decreases in virus infectivity that we observed. It will be interesting to determine

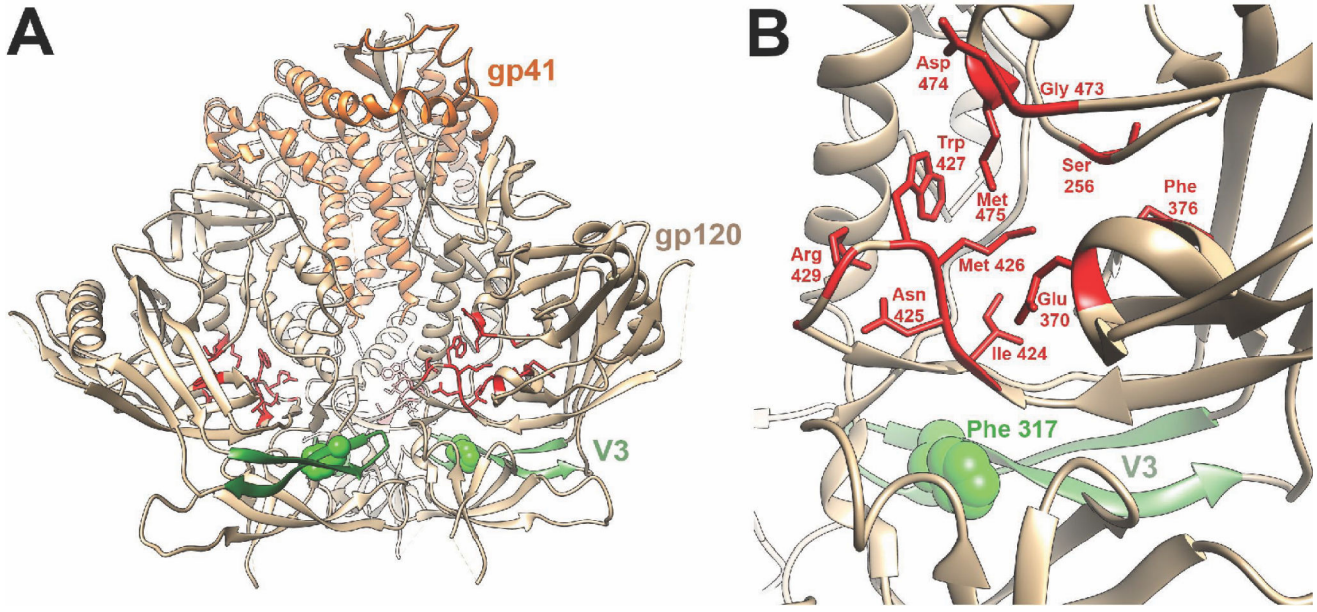

FIG 8 Relationship of the gp120 V3 loop and CD4mc binding site on an Env trimer structure. A side view of the unliganded HIV-1_{BG505} sgp140 SOSIP.664 Env trimer (PDB 4ZMJ) (85) is shown, with gp41 (orange) at the top and gp120 (tan) at the bottom of the image. The gp120 V3 loop is colored green, with residue 317 shown in CPK representation. The gp120 residues within 3.5 Angstroms of the CD4mc CJF-III-288 in gp120 core co-crystals (PDB 8FM3) (57) are colored red and shown in stick representation. (B) Close-up view of the gp120 region encompassing the V3 loop (with Phe 317) and the CJF-III-288 binding site, represented as in A. The CJF-III-288 contact residues (in red) are completely conserved between the A4 and BG505 Envs, as is Ser 375, which is not visible from this perspective. In a single protomer of the HIV-1_{BG505} sgp140 SOSIP.664 Env trimer, Phe 317 is 13.5 Angstroms from the nearest residue (Ile 424) that contacts CJF-III-288. Phe 317 on the adjacent Env protomer is even further away from the CJF-III-288 binding site.

how various properties associated with Env triggerability are related in a larger panel of primary HIV-1 strains.

Among primary HIV-1, sensitivity to inhibition by CD4mcs and soluble CD4 (sCD4) is only weakly correlated (57). Nonetheless, changes in Env triggerability have been shown to result in resistance to both CD4mcs and sCD4 (64, 66, 68). In light of the apparent ability of V3 changes to modulate Env triggerability, it is interesting that V3 sequences from primary HIV-1 strains are major determinants of sCD4 sensitivity (86).

Changes in the gp120 Phe-43 cavity that affected HIV-1 sensitivity to both CD4mcs and BMS-806 arose during selection of a BNM-III-170-resistant virus (62). By contrast, the alterations of the V3 loop observed here affected sensitivity to CD4mcs but not to BMS-806. Unlike CD4mcs, conformational blockers like BMS-806 and its analogs do not need to induce large-scale conformational changes in Env to exert their antiviral effect (12). As a result, the potency of BMS-806 analogs is less susceptible to Env alterations distant from the drug-binding site that alter triggerability. Thus, despite the proximity of the gp120 binding sites of CD4mcs and BMS-806 (87, 88), the distinct consequences of binding related to their antiviral mechanisms strongly impact potential HIV-1 pathways of resistance. An appreciation of the differences between these classes of gp120-directed virus entry inhibitors will guide potential applications.

MATERIALS AND METHODS

Plasmids

The *env* genes encoding the A4 and BG505 Envs and chimeric Envs were expressed using the pcDNA3.1 Env plasmid (GenBank accession numbers QPJ74671 for the A4 *env* and ABA61516 for the BG505 *env*). Chimeric Envs were constructed by Q5 site-directed mutagenesis (New England BioLabs). The $gp120_Bgp41_A$ chimera has the gp120 region of BG505 (**5**′atgagagtgatggggatacaga….. aagagtggtggggagagaaaaaaga**3**′) and the gp41 sequence of A4 (**5**′gcagttgttggaatggg……. ttgaaagggctttactataa**3**′). The $gp120_Agp41_B$ chimera has the gp120 region of A4 (**5**′atgagagcgagggggacaca….. aagagtggtgggaagaggaaaaaga**3**′) and the gp41 of BG505 (**5**′gcagttggaataggagctgtcttcct……. tcagacagggcctcgaaagggctttgctataa**3**′).

In $B(V1/V2+gp41)_A$, the V1V2 region (**5**′tgtaccaatgtcaccaataatat….. aacaaggagtatagattaataaattgt**3**′) of $gp120_Bgp41_A$ is replaced by the V1V2 region (**5**′tgtatcgatattgccaatgacacaagccgcaatg……. ttagtaataatagcagtgagtatagattaataaattgt**3**′) of A4. In $B(V3+gp41)_A$, the V3 region (**5**′tgtaccagacctaacaacaatacaagg ……. taggggatataagacaagcacattgt**3**′) of $gp120_Bgp41_A$ is replaced by the V3 region (**5**′ tgtactagacctggcaataataca……. ataataggggatataagacaagcatattgt**3**′) of A4.

In $A(N\text{-}gp120)_B$, the N terminus (**5**′atgagagcgagggggacacagaagaat…….. ataataggggatataagacaagcatattgt**3**′) of A4 gp120 is replaced by the N terminus (**5**′atgagagtgatggggatacagaggaattgtcag……taggggatataagacaagcacattgt**3**′) of BG505 gp120.

In $A(C\text{-}gp120)_B$, the C terminus (**5**′tgtactagacctggcaataataca……aaggagaagagtggtgggaagaggaaaaaga**3**′) of A4 gp120 is replaced by the C terminus (**5**′tgtaccagacctaacaacaatacaagg……. caaagagaagagtggtggggagagaaaaaaga**3**′) of BG505 gp120.

Additional primary HIV-1 Envs included in this study are from $HIV\text{-}1_{191084}$ and $HIV\text{-}1_{AG253.11}$ (GenBank accession numbers ADI62025 and ACC97453, respectively).

For experiments in which the Envs were expressed in the context of an HIV-1 provirus, the *env* genes were cloned into the pNL4-3 proviral clone (89). Using Q5 site-directed mutagenesis, NheI and SalI restriction sites were introduced into the pNL4-3 plasmid before the start and end of the *env* gene, respectively, using the primers (Fp: tacgta*cccggg*atgggtggcaagtggtcaaaaagtagtgt and Rp: atagta*gctagc*tgccactgtcttctgctctttctattagtct). The resulting construct was named pNL4 5′NheI-3′SmaI. Using the primers (A4FpNheI: atagtagctagcatgagagcgaggggacaca, A4RpSmaI: tacgtacccgggttatagtaaagccctttcaaaaccctgc and BG505FpNheI: atagtagctagcatgagagtgatggggatacaga, BG505RpSmaI: tacgtacccgggttatagcaaagccctttcgagg) and PfuUltra II DNA Polymerase (Agilent), A4 and BG505 sequences were amplified,

introducing NheI and SmaI restriction sites at their 5′ and 3′ ends, respectively. The amplified BG505 and A4 PCR products and pNL4 5′NheI-3′SmaI were digested with NheI and SmaI restriction enzymes and then ligated to yield the constructs pNL4-3 NheIBG505SmaI and pNL4-3 NheIA4SmaI, respectively.

Using site-directed mutagenesis, the NheI (A4Fp: atgagagcgagggggacaca, BG505Fp: atgagagtgatggggatacaga, Rp: tgccactgtcttctgctctttcta) and SmaI (Fp: gatgggtgg-caagtggtcaaaaagtagtgtgattgga, RpA4: ttatagtaaagccctttcaaaaccctg, BG505Rp: ttatag-caaagccctttcgaggccctgtctgatt) restriction sites were removed to yield pNL4-3.A4 and pNL4-3.BG505. The DNA sequence of the *env* gene was confirmed for all constructs.

Cell lines and primary cells

293T cells were grown in Dulbecco's Modified Eagle's medium (Life Technologies, Wisent, Inc.) supplemented with 10% fetal bovine serum (Life Technologies, VWR) and 100 µg/mL of penicillin-streptomycin (Life Technologies, Wisent, Inc.). Cf2Th-CD4/CCR5 cells stably expressing the human CD4 and CCR5 coreceptors for HIV-1 were grown in the same medium supplemented with 0.4 mg/mL of G418 and 0.2 mg/mL of hygromycin. Cf2Th-CCR5 cells stably expressing the CCR5 coreceptor of HIV-1 were grown in the same medium supplemented with 0.4 mg/mL of G418.

Small-molecule HIV-1 entry inhibitors

The CD4mcs BNM-III-170, CJF-III-192, and CJF-III-288 were synthesized as described previously (37, 57). The compounds were dissolved in dimethyl sulfoxide at a stock concentration of 10 mM and diluted to the appropriate concentration in cell culture medium for antiviral assays. BMS-806 was purchased from Selleckchem.

Expression and processing of HIV-1 Env variants

HEK 293T cells were transfected transiently with plasmids encoding Envs, HIV-1 packaging proteins, and a luciferase-expressing HIV-1 vector (26). Forty-eight hours later, the cell supernatant was cleared (600 × *g* for 10 min) followed by filtration through a 0.45-µm membrane. The viruses were pelleted by centrifugation at 14,000 × *g* for 1.5 hours at 4°C and lysed. The cell and virus lysates were Western blotted and probed with a goat polyclonal anti-gp120 antibody (Invitrogen), the 4E10 anti-gp41 antibody (NIH HIV Reagent Program), or a rabbit anti-Gag antibody (Abcam). The cell lysates were also Western blotted and probed with a rabbit anti-hsp70 antibody (Santa Cruz).

Production of recombinant pseudoviruses expressing luciferase

As described previously (26), 293T cells were transfected with pSVIIIenv plasmids expressing Env variants, the pCMVΔP1Δenv HIV-1 Gag-Pol packaging construct, and the firefly luciferase-expressing HIV-1 vector at a 1:1:3 µg DNA ratio using effectene transfection reagent (Qiagen). Recombinant, luciferase-expressing viruses capable of a single round of replication were released into the cell medium and were harvested 48 h later. The virus-containing supernatants were clarified by low-speed centrifugation (600 × *g* for 10 min) and used for single-round infections.

Virus infectivity, inhibition, and cold sensitivity

Single-round virus infection assays were used to measure the ability of the Env variants to support virus entry, as described previously (26). To measure the infectivity of the Env pseudotypes, equal volumes of HEK 293T cell supernatants containing recombinant viruses were added to Cf2Th-CD4/CCR5 target cells expressing CD4 and CCR5. Forty-eight hours later, the target cells were lysed and the luciferase activity was measured. In parallel, aliquots of the virus-containing HEK 293T cell supernatants were processed and analyzed by Western blotting, as described above.

To measure virus inhibition, the compounds to be tested were incubated with pseudoviruses for 1 hour at 37°C. The mixture was then added to Cf2Th-CD4/CCR5 target

cells expressing CD4 and CCR5. Forty-eight hours later, the target cells were lysed, and the luciferase activity was measured.

To evaluate the cold sensitivity of the Env variants, pseudotyped recombinant viruses were incubated on ice for various lengths of time prior to measuring their infectivity, as described previously (26, 27, 63, 64, 79).

gp120 shedding

To measure CD4mc-induced gp120 shedding, 293T cells were transfected transiently with pNL4-3 provirus constructs expressing the A4, BG505, $A(307)_B$, $A(317)_B$, $B(317)_A$, and $B(307+317)_A$ Envs. The transfected cell supernatants were harvested 48 hours later, clarified by low-speed centrifugation (600 × *g* for 10 min) and filtered through a 0.45-µm membrane. The viruses were pelleted by centrifugation at 14,000 × *g* for 1.5 hours at 4°C and resuspended in 100 µL of 1× phosphate-buffered saline (PBS). The viruses were incubated with different concentrations of CJF-III-288 for 2.5 hours at 37°C, followed by centrifugation at 14,000 × *g* for 1.5 hours at 4°C. The virus pellets were lysed in 1× lithium dodecyl sulfate (LDS) buffer. The supernatants containing shed gp120 were bound to Galanthus nivalis lectin beads (Thermo Fisher Scientific). The glycoproteins captured on the beads and the lysates of virus pellets were Western blotted and probed with a goat anti-gp120 antibody, a 4E10 anti-gp41 antibody, or a rabbit anti-Gag antibody. The Western blots were quantified using Image J software (90).

Activation of virus infection by CD4mcs

Pseudoviruses were incubated with CD4-negative, CCR5-expressing Cf2Th-CCR5 cells in 96-well plates. The plates were centrifuged at 600 × *g* for 30 min at 21°C. Medium containing serial dilutions of CD4mc was then added. Forty-eight hours later, cells were lysed, and luciferase activity was measured.

Statistics

The concentrations of HIV-1 entry inhibitors that inhibit 50% of infection (IC_{50} values) were determined by fitting the data in five-parameter dose-response curves using GraphPad Prism 8. Spearman rank-order correlation coefficients (r_S) and p values were calculated using VassarStats (91).

ACKNOWLEDGMENTS

We thank Ms. Elizabeth Carpelan for manuscript preparation. Antibodies against HIV-1 were kindly supplied by Dennis Burton (Scripps), Peter Kwong and John Mascola (Vaccine Research Center NIH), Barton Haynes (Duke University), Hermann Katinger (Polymun), James Robinson (Tulane University), and Marshall Posner (Mount Sinai Medical Center). We thank the NIH HIV Reagent Program for providing reagents.

This work was supported by grants from the National Institutes of Health (grants AI145547, AI124982, AI129017, AI164562, AI150471, AI148379, AI150322, AI129769, and AI176904), by an HIV Cure Research Grant from Gilead Sciences, and by a gift from the late William F. McCarty-Cooper.

AUTHOR AFFILIATIONS

[1]Department of Cancer Immunology and Virology, Dana-Farber Cancer Institute, Boston, Massachusetts, USA
[2]Department of Microbiology, Harvard Medical School, Boston, Massachusetts, USA
[3]Department of Chemistry, University of Pennsylvania, Philadelphia, Pennsylvania, USA

AUTHOR ORCIDs

Joseph Sodroski http://orcid.org/0000-0002-9750-1615

FUNDING

Funder	Grant(s)	Author(s)
HHS | National Institutes of Health (NIH)	AI145547	Joseph Sodroski
HHS | National Institutes of Health (NIH)	AI124982	Joseph Sodroski
HHS | National Institutes of Health (NIH)	AI129017	Joseph Sodroski
HHS | National Institutes of Health (NIH)	AI164562	Joseph Sodroski
HHS | National Institutes of Health (NIH)	AI150471	Joseph Sodroski
HHS | National Institutes of Health (NIH)	AI176904	Joseph Sodroski
HHS | National Institutes of Health (NIH)	AI148379	Amos B. Smith III Joseph Sodroski
HHS | National Institutes of Health (NIH)	AI150322	Amos B. Smith III Joseph Sodroski
HHS | National Institutes of Health (NIH)	AI129769	Amos B. Smith III Joseph Sodroski

REFERENCES

1. Wyatt R, Sodroski J. 1998. The HIV-1 envelope glycoproteins: fusogens, antigens, and immunogens. Science 280:1884–1888. https://doi.org/10.1126/science.280.5371.1884
2. Klatzmann D, Champagne E, Chamaret S, Gruest J, Guetard D, Hercend T, Gluckman JC, Montagnier L. 1984. T-lymphocyte T4 molecule behaves as the receptor for human retrovirus LAV. Nature 312:767–768. https://doi.org/10.1038/312767a0
3. Dalgleish AG, Beverley PC, Clapham PR, Crawford DH, Greaves MF, Weiss RA. 1984. The CD4 (T4) antigen is an essential component of the receptor for the AIDS retrovirus. Nature 312:763–767. https://doi.org/10.1038/312763a0
4. Wu L, Gerard NP, Wyatt R, Choe H, Parolin C, Ruffing N, Borsetti A, Cardoso AA, Desjardin E, Newman W, Gerard C, Sodroski J. 1996. CD4-induced interaction of primary HIV-1 gp120 glycoproteins with the chemokine receptor CCR-5. Nature 384:179–183. https://doi.org/10.1038/384179a0
5. Trkola A, Dragic T, Arthos J, Binley JM, Olson WC, Allaway GP, Cheng-Mayer C, Robinson J, Maddon PJ, Moore JP. 1996. CD4-dependent, antibody-sensitive interactions between HIV-1 and its co-receptor CCR-5. Nature 384:184–187. https://doi.org/10.1038/384184a0
6. Choe H, Farzan M, Sun Y, Sullivan N, Rollins B, Ponath PD, Wu L, Mackay CR, LaRosa G, Newman W, Gerard N, Gerard C, Sodroski J. 1996. The beta-chemokine receptors CCR3 and CCR5 facilitate infection by primary HIV-1 isolates. Cell 85:1135–1148. https://doi.org/10.1016/s0092-8674(00)81313-6
7. Deng H, Liu R, Ellmeier W, Choe S, Unutmaz D, Burkhart M, Di Marzio P, Marmon S, Sutton RE, Hill CM, Davis CB, Peiper SC, Schall TJ, Littman DR, Landau NR. 1996. Identification of a major co-receptor for primary isolates of HIV-1. Nature 381:661–666. https://doi.org/10.1038/381661a0
8. Dragic T, Litwin V, Allaway GP, Martin SR, Huang Y, Nagashima KA, Cayanan C, Maddon PJ, Koup RA, Moore JP, Paxton WA. 1996. HIV-1 entry into CD4+ cells is mediated by the chemokine receptor CC-CKR-5. Nature 381:667–673. https://doi.org/10.1038/381667a0
9. Doranz BJ, Rucker J, Yi Y, Smyth RJ, Samson M, Peiper SC, Parmentier M, Collman RG, Doms RW. 1996. A dual-tropic primary HIV-1 isolate that uses fusin and the beta-chemokine receptors CKR-5, CKR-3, and CKR-2B as fusion cofactors. Cell 85:1149–1158. https://doi.org/10.1016/S0092-8674(00)81314-8
10. Feng Y, Broder CC, Kennedy PE, Berger EA. 1996. HIV-1 entry cofactor: functional cDNA cloning of a seven-transmembrane, G protein-coupled receptor. Science 272:872–877. https://doi.org/10.1126/science.272.5263.872
11. Alkhatib G, Combadiere C, Broder CC, Feng Y, Kennedy PE, Murphy PM, Berger EA. 1996. CC CKR5: a RANTES, MIP-1alpha, MIP-1beta receptor as a fusion cofactor for macrophage-tropic HIV-1. Science 272:1955–1958. https://doi.org/10.1126/science.272.5270.1955
12. Munro JB, Gorman J, Ma X, Zhou Z, Arthos J, Burton DR, Koff WC, Courter JR, Smith AB, Kwong PD, Blanchard SC, Mothes W. 2014. Conformational dynamics of single HIV-1 envelope trimers on the surface of native virions. Science 346:759–763. https://doi.org/10.1126/science.1254426
13. Herschhorn A, Ma X, Gu C, Ventura JD, Castillo-Menendez L, Melillo B, Terry DS, Smith AB, Blanchard SC, Munro JB, Mothes W, Finzi A, Sodroski J. 2016. Release of gp120 restraints leads to an entry-competent intermediate state of the HIV-1 envelope glycoproteins. mBio 7:e01598-16. https://doi.org/10.1128/mBio.01598-16
14. Ma X, Lu M, Terry DS, Gorman J, Kwong PD, Blanchard SC, Munro JB, Mothes W. 2017. Single-molecule FRET delineates asymmetric trimer conformations during HIV-1 entry. Biophys J 112:177a. https://doi.org/10.1016/j.bpj.2016.11.980
15. Lu M, Ma X, Reichard N, Terry DS, Arthos J, Smith AB, Sodroski JG, Blanchard SC, Mothes W. 2020. Shedding-resistant HIV-1 envelope glycoproteins adopt downstream conformations that remain responsive to conformation-preferring ligands. J Virol 94:e00597-20. https://doi.org/10.1128/JVI.01661-20
16. Furuta RA, Wild CT, Weng Y, Weiss CD. 1998. Capture of an early fusion-active conformation of HIV-1 gp41. Nat Struct Biol 5:276–279. https://doi.org/10.1038/nsb0498-276
17. Koshiba T, Chan DC. 2003. The prefusogenic intermediate of HIV-1 gp41 contains exposed C-peptide regions. J Biol Chem 278:7573–7579. https://doi.org/10.1074/jbc.M211154200
18. He Y, Vassell R, Zaitseva M, Nguyen N, Yang Z, Weng Y, Weiss CD. 2003. Peptides trap the human immunodeficiency virus type 1 envelope glycoprotein fusion intermediate at two sites. J Virol 77:1666–1671. https://doi.org/10.1128/jvi.77.3.1666-1671.2003
19. Si Z, Madani N, Cox JM, Chruma JJ, Klein JC, Schön A, Phan N, Wang L, Biorn AC, Cocklin S, Chaiken I, Freire E, Smith AB, Sodroski JG. 2004. Small-molecule inhibitors of HIV-1 entry block receptor-induced conformational changes in the viral envelope glycoproteins. Proc Natl Acad Sci U S A 101:5036–5041. https://doi.org/10.1073/pnas.0307953101
20. Chan DC, Fass D, Berger JM, Kim PS. 1997. Core structure of gp41 from the HIV envelope glycoprotein. Cell 89:263–273. https://doi.org/10.1016/s0092-8674(00)80205-6
21. Weissenhorn W, Dessen A, Harrison SC, Skehel JJ, Wiley DC. 1997. Atomic structure of the ectodomain from HIV-1 gp41. Nature 387:426–430. https://doi.org/10.1038/387426a0
22. Lu M, Blacklow SC, Kim PS. 1995. A trimeric structural domain of the HIV-1 transmembrane glycoprotein. Nat Struct Biol 2:1075–1082. https://doi.org/10.1038/nsb1295-1075
23. Wilen CB, Tilton JC, Doms RW. 2012. Molecular mechanisms of HIV entry. Adv Exp Med Biol 726:223–242. https://doi.org/10.1007/978-1-4614-0980-9_10

24. Melikyan GB, Markosyan RM, Hemmati H, Delmedico MK, Lambert DM, Cohen FS. 2000. Evidence that the transition of HIV-1 gp41 into a six-helix bundle, not the bundle configuration, induces membrane fusion. J Cell Biol 151:413–423. https://doi.org/10.1083/jcb.151.2.413
25. Kuhmann SE, Platt EJ, Kozak SL, Kabat D. 2000. Cooperation of multiple CCR5 coreceptors is required for infections by human immunodeficiency virus type 1. J Virol 74:7005–7015. https://doi.org/10.1128/jvi.74.15.7005-7015.2000
26. Haim H, Strack B, Kassa A, Madani N, Wang L, Courter JR, Princiotto A, McGee K, Pacheco B, Seaman MS, Smith AB, Sodroski J. 2011. Contribution of intrinsic reactivity of the HIV-1 envelope glycoproteins to CD4-independent infection and global inhibitor sensitivity. PLoS Pathog 7:e1002101. https://doi.org/10.1371/journal.ppat.1002101
27. Haim H, Salas I, McGee K, Eichelberger N, Winter E, Pacheco B, Sodroski J. 2013. Modeling virus- and antibody-specific factors to predict human immunodeficiency virus neutralization efficiency. Cell Host Microbe 14:547–558. https://doi.org/10.1016/j.chom.2013.10.006
28. Guttman M, Cupo A, Julien JP, Sanders RW, Wilson IA, Moore JP, Lee KK. 2015. Antibody potency relates to the ability to recognize the closed, pre-fusion form of HIV Env. Nat Commun 6:6144. https://doi.org/10.1038/ncomms7144
29. Kwong PD, Doyle ML, Casper DJ, Cicala C, Leavitt SA, Majeed S, Steenbeke TD, Venturi M, Chaiken I, Fung M, Katinger H, Parren P, Robinson J, Van Ryk D, Wang L, Burton DR, Freire E, Wyatt R, Sodroski J, Hendrickson WA, Arthos J. 2002. HIV-1 evades antibody-mediated neutralization through conformational masking of receptor-binding sites. Nature 420:678–682. https://doi.org/10.1038/nature01188
30. Kwong P.D, Wyatt R, Robinson J, Sweet RW, Sodroski J, Hendrickson WA. 1998. Structure of an HIV gp120 envelope glycoprotein in complex with the CD4 receptor and a neutralizing human antibody. Nature 393:648–659. https://doi.org/10.1038/31405
31. Schön A, Madani N, Klein JC, Hubicki A, Ng D, Yang X, Smith AB, Sodroski J, Freire E. 2006. Thermodynamics of binding of a low-molecular-weight CD4 mimetic to HIV-1 gp120. Biochemistry 45:10973–10980. https://doi.org/10.1021/bi061193r
32. Herschhorn A, Gu C, Espy N, Richard J, Finzi A, Sodroski JG. 2014. A broad HIV-1 inhibitor blocks envelope glycoprotein transitions critical for entry. Nat Chem Biol 10:845–852. https://doi.org/10.1038/nchembio.1623
33. Madani N, Perdigoto AL, Srinivasan K, Cox JM, Chruma JJ, LaLonde J, Head M, Smith AB, Sodroski JG. 2004. Localized changes in the gp120 envelope glycoprotein confer resistance to human immunodeficiency virus entry inhibitors BMS-806 and #155. J Virol 78:3742–3752. https://doi.org/10.1128/jvi.78.7.3742-3752.2004
34. Pancera M, Lai Y-T, Bylund T, Druz A, Narpala S, O'Dell S, Schön A, Bailer RT, Chuang G-Y, Geng H, Louder MK, Rawi R, Soumana DI, Finzi A, Herschhorn A, Madani N, Sodroski J, Freire E, Langley DR, Mascola JR, McDermott AB, Kwong PD. 2017. Crystal structures of trimeric HIV envelope with entry inhibitors BMS-378806 and BMS-626529. Nat Chem Biol 13:1115–1122. https://doi.org/10.1038/nchembio.2460
35. Madani N, Schön A, Princiotto AM, Lalonde JM, Courter JR, Soeta T, Ng D, Wang L, Brower ET, Xiang S-H, Kwon YD, Huang C-C, Wyatt R, Kwong PD, Freire E, Smith AB, Sodroski J. 2008. Small-molecule CD4 mimics interact with a highly conserved pocket on HIV-1 gp120. Structure 16:1689–1701. https://doi.org/10.1016/j.str.2008.09.005
36. Kwon YD, LaLonde JM, Yang Y, Elban MA, Sugawara A, Courter JR, Jones DM, Smith AB, Debnath AK, Kwong PD. 2014. Crystal structures of HIV-1 gp120 envelope glycoprotein in complex with NBD analogues that target the CD4-binding site. PLoS One 9:e85940. https://doi.org/10.1371/journal.pone.0085940
37. Melillo B, Liang S, Park J, Schön A, Courter JR, LaLonde JM, Wendler DJ, Princiotto AM, Seaman MS, Freire E, Sodroski J, Madani N, Hendrickson WA, Smith AB. 2016. Small-molecule CD4-mimics: structure-based optimization of HIV-1 entry inhibition. ACS Med Chem Lett 7:330–334. https://doi.org/10.1021/acsmedchemlett.5b00471
38. Curreli F, Kwon YD, Belov DS, Ramesh RR, Kurkin AV, Altieri A, Kwong PD, Debnath AK. 2017. Synthesis, antiviral potency, *in vitro* ADMET, and X-ray structure of potent CD4 mimics as entry inhibitors that target the Phe43 cavity of HIV-1 gp120. J Med Chem 60:3124–3153. https://doi.org/10.1021/acs.jmedchem.7b00690
39. Herschhorn A, Gu C, Moraca F, Ma X, Farrell M, Smith AB, Pancera M, Kwong PD, Schön A, Freire E, Abrams C, Blanchard SC, Mothes W, Sodroski JG. 2017. The β20-β21 of gp120 is a regulatory switch for HIV-1 Env conformational transitions. Nat Commun 8:1049. https://doi.org/10.1038/s41467-017-01119-w
40. Zhao Q, Ma L, Jiang S, Lu H, Liu S, He Y, Strick N, Neamati N, Debnath AK. 2005. Identification of N-phenyl-N'-(2,2,6,6-tetramethyl-piperidin-4-yl)-oxalamides as a new class of HIV-1 entry inhibitors that prevent gp120 binding to CD4. Virology 339:213–225. https://doi.org/10.1016/j.virol.2005.06.008
41. Haim H, Si Z, Madani N, Wang L, Courter JR, Princiotto A, Kassa A, DeGrace M, McGee-Estrada K, Mefford M, Gabuzda D, Smith AB, Sodroski J. 2009. Soluble CD4 and CD4-mimetic compounds inhibit HIV-1 infection by induction of a short-lived activated state. PLoS Pathog 5:e1000360. https://doi.org/10.1371/journal.ppat.1000360
42. Madani N, Princiotto AM, Zhao C, Jahanbakhshsefidi F, Mertens M, Herschhorn A, Melillo B, Smith AB, Sodroski J. 2017. Activation and inactivation of primary human immunodeficiency virus envelope glycoprotein trimers by CD4-mimetic compounds. J Virol 91:e01880-16. https://doi.org/10.1128/JVI.01880-16
43. Madani N, Princiotto AM, Mach L, Ding S, Prevost J, Richard J, Hora B, Sutherland L, Zhao CA, Conn BP, Bradley T, Moody MA, Melillo B, Finzi A, Haynes BF, Smith III AB, Santra S, Sodroski J. 2018. A CD4-mimetic compound enhances vaccine efficacy against stringent immunodeficiency virus challenge. Nat Commun 9:2363. https://doi.org/10.1038/s41467-018-04758-9
44. Yoshimura K, Harada S, Shibata J, Hatada M, Yamada Y, Ochiai C, Tamamura H, Matsushita S. 2010. Enhanced exposure of human immunodeficiency virus type 1 primary isolate neutralization epitopes through binding of CD4 mimetic compounds. J Virol 84:7558–7568. https://doi.org/10.1128/JVI.00227-10
45. Madani N, Princiotto AM, Schön A, LaLonde J, Feng Y, Freire E, Park J, Courter JR, Jones DM, Robinson J, Liao H-X, Moody MA, Permar S, Haynes B, Smith AB, Wyatt R, Sodroski J. 2014. CD4-mimetic small molecules sensitize human immunodeficiency virus to vaccine-elicited antibodies. J Virol 88:6542–6555. https://doi.org/10.1128/JVI.00540-14
46. Richard J, Pacheco B, Gohain N, Veillette M, Ding S, Alsahafi N, Tolbert WD, Prévost J, Chapleau J-P, Coutu M, Jia M, Brassard N, Park J, Courter JR, Melillo B, Martin L, Tremblay C, Hahn BH, Kaufmann DE, Wu X, Smith AB, Sodroski J, Pazgier M, Finzi A. 2016. Co-receptor binding site antibodies enable CD4-mimetics to expose conserved anti-cluster A ADCC epitopes on HIV-1 envelope glycoproteins. EBioMedicine 12:208–218. https://doi.org/10.1016/j.ebiom.2016.09.004
47. Alsahafi N, Bakouche N, Kazemi M, Richard J, Ding S, Bhattacharyya S, Das D, Anand SP, Prévost J, Tolbert WD, Lu H, Medjahed H, Gendron-Lepage G, Ortega Delgado GG, Kirk S, Melillo B, Mothes W, Sodroski J, Smith AB, Kaufmann DE, Wu X, Pazgier M, Rouiller I, Finzi A, Munro JB. 2019. An asymmetric opening of HIV-1 envelope mediates antibody-dependent cellular cytotoxicity. Cell Host Microbe 25:578–587. https://doi.org/10.1016/j.chom.2019.03.002
48. Richard J, Veillette M, Brassard N, Iyer SS, Roger M, Martin L, Pazgier M, Schön A, Freire E, Routy J-P, Smith AB, Park J, Jones DM, Courter JR, Melillo BN, Kaufmann DE, Hahn BH, Permar SR, Haynes BF, Madani N, Sodroski JG, Finzi A. 2015. CD4 mimetics sensitize HIV-1-infected cells to ADCC. Proc Natl Acad Sci U S A 112:E2687–E2694. https://doi.org/10.1073/pnas.1506755112
49. Ding S, Verly MM, Princiotto A, Melillo B, Moody AM, Bradley T, Easterhoff D, Roger M, Hahn BH, Madani N, Smith AB, Haynes BF, Sodroski J, Finzi A. 2017. Short communication: small-molecule CD4 mimetics sensitize HIV-1-infected cells to antibody-dependent cellular cytotoxicity by antibodies elicited by multiple envelope glycoprotein immunogens in nonhuman primates. AIDS Res Hum Retroviruses 33:428–431. https://doi.org/10.1089/AID.2016.0246
50. Ding S, Grenier MC, Tolbert WD, Vézina D, Sherburn R, Richard J, Prévost J, Chapleau J-P, Gendron-Lepage G, Medjahed H, Abrams C, Sodroski J, Pazgier M, Smith AB, Finzi A. 2019. A new family of small-molecule CD4-mimetic compounds contacts highly conserved aspartic acid 368 of HIV-1 gp120 and mediates antibody-dependent cellular cytotoxicity. J Virol 93:e01325-19. https://doi.org/10.1128/JVI.01325-19
51. Rajashekar JK, Richard J, Beloor J, Prévost J, Anand SP, Beaudoin-Bussières G, Shan L, Herndler-Brandstetter D, Gendron-Lepage G, Medjahed H, et al. 2021. Modulating HIV-1 envelope glycoprotein conformation to decrease the HIV-1 reservoir. Cell Host Microbe 29:904–916. https://doi.org/10.1016/j.chom.2021.04.014

52. Princiotto AM, Vrbanac VD, Melillo B, Park J, Tager AM, Smith AB, Sodroski J, Madani N. 2018. A small-molecule CD4-mimetic compound protects bone marrow-liver-thymus humanized mice from HIV-1 infection. J Infect Dis 218:471–475. https://doi.org/10.1093/infdis/jiy174
53. Curreli F, Kwon YD, Zhang H, Yang Y, Scacalossi D, Kwong PD, Debnath AK. 2014. Binding mode characterization of NBD series CD4-mimetic HIV-1 entry inhibitors by X-ray structure and resistance study. Antimicrob Agents Chemother 58:5478–5491. https://doi.org/10.1128/AAC.03339-14
54. LaLonde JM, Kwon YD, Jones DM, Sun AW, Courter JR, Soeta T, Kobayashi T, Princiotto AM, Wu X, Schön A, Freire E, Kwong PD, Mascola JR, Sodroski J, Madani N, Smith AB. 2012. Structure-based design, synthesis, and characterization of dual Hotspot small-molecule HIV-1 entry inhibitors. J Med Chem 55:4382–4396. https://doi.org/10.1021/jm300265j
55. Courter JR, Madani N, Sodroski J, Schön A, Freire E, Kwong PD, Hendrickson WA, Chaiken IM, LaLonde JM, Smith AB. 2014. Structure-based design, synthesis and validation of CD4-mimetic small molecule inhibitors of HIV-1 entry: conversion of a viral entry agonist to an antagonist. Acc Chem Res 47:1228–1237. https://doi.org/10.1021/ar4002735
56. Ding S, Tolbert WD, Zhu H, Lee D, Marchitto L, Higgins T, Zhao X, Nguyen D, Sherburn R, Richard J, Gendron-Lepage G, Medjahed H, Mohammadi M, Abrams C, Pazgier M, Smith AB, Finzi A. 2023. Piperidine CD4-mimetic compounds expose vulnerable Env epitopes sensitizing HIV-1-infected cells to ADCC. bioRxiv 15:1185. https://doi.org/10.1101/2023.03.23.533923
57. Fritschi CJ, Anang S, Gong Z, Mohammadi M, Richard J, Bourassa C, Severino KT, Richter H, Yang D, Chen H-C, Chiu T-J, Seaman MS, Madani N, Abrams C, Finzi A, Hendrickson WA, Sodroski JG, Smith AB. 2023. Indoline CD4-mimetic compounds mediate potent and broad HIV-1 inhibition and sensitization to antibody-dependent cellular cytotoxicity. Proc Natl Acad Sci U S A 120:e2222073120. https://doi.org/10.1073/pnas.2222073120
58. Zoubchenok D, Veillette M, Prévost J, Sanders-Buell E, Wagh K, Korber B, Chenine AL, Finzi A. 2017. Histidine 375 modulates CD4 binding in HIV-1 CRF01_AE envelope glycoproteins. J Virol 91:e02151-16. https://doi.org/10.1128/JVI.02151-16
59. Foley, Apetrei C, Hahn B, Mizrachi I, Mullins J, Rambaut A, Wolinsky S, Korber B, eds. 2014. LA-UR-14-26717. HIV sequence compendium 2014. Los Alamos National Laboratory, Theoretical Biology and Biophysics, Los Alamos, NM.
60. Davey NE, Satagopam VP, Santiago-Mozos S, Villacorta-Martin C, Bharat TAM, Schneider R, Briggs JAG. 2014. The HIV mutation browser: a resource for human immunodeficiency virus mutagenesis and polymorphism data. PLoS Comput Biol 10:e1003951. https://doi.org/10.1371/journal.pcbi.1003951
61. Prévost J, Tolbert WD, Medjahed H, Sherburn RT, Madani N, Zoubchenok D, Gendron-Lepage G, Gaffney AE, Grenier MC, Kirk S, et al. 2020. The HIV-1 Env gp120 inner domain shapes the Phe43 cavity and the CD4 binding site. mBio 11:e00280-20. https://doi.org/10.1128/mBio.00280-20
62. Anang S, Richard J, Bourassa C, Goyette G, Chiu T-J, Chen H-C, Smith AB, Madani N, Finzi A, Sodroski J. 2022. Characterization of human immunodeficiency virus (HIV-1) envelope glycoprotein variants selected for resistance to a CD4-mimetic compound. J Virol 96:e0063622. https://doi.org/10.1128/jvi.00636-22
63. Kassa A, Madani N, Schön A, Haim H, Finzi A, Xiang S-H, Wang L, Princiotto A, Pancera M, Courter J, Smith AB, Freire E, Kwong PD, Sodroski J. 2009. Transitions to and from the CD4-bound conformation are modulated by a single-residue change in the human immunodeficiency virus type 1 gp120 inner domain. J Virol 83:8364–8378. https://doi.org/10.1128/JVI.00594-09
64. Nguyen HT, Qualizza A, Anang S, Zhao M, Zou S, Zhou R, Wang Q, Zhang S, Deshpande A, Ding H, Chiu T-J, Smith AB, Kappes JC, Sodroski JG. 2022. Functional and highly cross-linkable HIV-1 envelope glycoproteins enriched in a pretriggered conformation. J Virol 96:e0166821. https://doi.org/10.1128/jvi.01668-21
65. Finzi A, Xiang S-H, Pacheco B, Wang L, Haight J, Kassa A, Danek B, Pancera M, Kwong PD, Sodroski J. 2010. Topological layers in the HIV-1 gp120 inner domain regulate gp41 interaction and CD4-triggered conformational transitions. Mol Cell 37:656–667. https://doi.org/10.1016/j.molcel.2010.02.012
66. Pacheco B, Alsahafi N, Debbeche O, Prévost J, Ding S, Chapleau J-P, Herschhorn A, Madani N, Princiotto A, Melillo B, Gu C, Zeng X, Mao Y, Smith AB, Sodroski J, Finzi A. 2017. Residues in the gp41 ectodomain regulate HIV-1 envelope glycoprotein conformational transitions induced by gp120-directed inhibitors. J Virol 91:e02219-16. https://doi.org/10.1128/JVI.02219-16
67. Jette CA, Barnes CO, Kirk SM, Melillo B, Smith AB, Bjorkman PJ. 2021. Cryo-EM structures of HIV-1 Trimer bound to CD4-mimetics BNM-III-170 and M48U1 adopt a CD4-bound open conformation. Nat Commun 12:1950. https://doi.org/10.1038/s41467-021-21816-x
68. Wang Q, Esnault F, Zhao M, Chiu T-J, Smith AB, Nguyen HT, Sodroski JG. 2022. Global increases in human immunodeficiency virus neutralization sensitivity due to alterations in the membrane-proximal external region of the envelope glycoprotein can be minimized by distant state 1-stabilizing changes. J Virol 96:e0187821. https://doi.org/10.1128/jvi.01878-21
69. Gnanakaran S, Daniels MG, Bhattacharya T, Lapedes AS, Sethi A, Li M, Tang H, Greene K, Gao H, Haynes BF, Cohen MS, Shaw GM, Seaman MS, Kumar A, Gao F, Montefiori DC, Korber B. 2010. Genetic signatures in the envelope glycoproteins of HIV-1 that associate with broadly neutralizing antibodies. PLoS Comput Biol 6:e1000955. https://doi.org/10.1371/journal.pcbi.1000955
70. Balinda SN, Kapaata A, Xu R, Salazar MG, Mezzell AT, Qin Q, Herard K, Dilernia D, Kamali A, Ruzagira E, Kibengo FM, Song H, Ochsenbauer C, Salazar-Gonzalez JF, Gilmour J, Hunter E, Yue L, Kaleebu P. 2022. Characterization of near full-length transmitted/founder HIV-1 subtype D and A/D recombinant genomes in a heterosexual ugandan population (2006-2011). Viruses 14:334. https://doi.org/10.3390/v14020334
71. Wu X, Parast AB, Richardson BA, Nduati R, John-Stewart G, Mbori-Ngacha D, Rainwater SMJ, Overbaugh J. 2006. Neutralization escape variants of human immunodeficiency virus type 1 are transmitted from mother to infant. J Virol 80:835–844. https://doi.org/10.1128/JVI.80.2.835-844.2006
72. Huang C, Tang M, Zhang M-Y, Majeed S, Montabana E, Stanfield RL, Dimitrov DS, Korber B, Sodroski J, Wilson IA, Wyatt R, Kwong PD. 2005. Structure of a V3-containing HIV-1 gp120 core. Science 310:1025–1028. https://doi.org/10.1126/science.1118398
73. Korber BT, Foley BT, Kuiken CL, Pillai SK, Sodroski JG. 1998. Numbering positions in HIV relative to HXB2CG. Available from: https://hfv.lanl.gov/content/sequence/HIV/COMPENDIUM/1998/III/HXB2.pdf
74. Imamichi H, Koita O, Dabitao D, Dao S, Ibrah M, Sogoba D, Dewar RL, Berg SC, Jiang M-K, Parta M, Washington JA, Polis MA, Lane HC, Tounkara A. 2009. Identification and characterization of CRF02_AG, CRF06_cpx, and CRF09_cpx recombinant subtypes in Mali, West Africa. AIDS Res Hum Retroviruses 25:45–55. https://doi.org/10.1089/aid.2008.0111
75. Jacob RA, Abrahams F, Tongo M, Schomaker M, Roux P, Mpoudi Ngole E, Burgers WA, Dorfman JR. 2012. Refined identification of neutralization-resistant HIV-1 CRF02_AG viruses. J Virol 86:7699–7703. https://doi.org/10.1128/JVI.00804-12
76. Bagaya BS, Tian M, Nickel GC, Vega JF, Li Y, He P, Klein K, Mann JFS, Jiang W, Arts EJ, Gao Y. 2017. An *in vitro* model to mimic selection of replication-competent HIV-1 intersubtype recombination in dual or superinfected patients. J Mol Biol 429:2246–2264. https://doi.org/10.1016/j.jmb.2017.04.016
77. de Taeye SW, Ozorowski G, Torrents de la Peña A, Guttman M, Julien J-P, van den Kerkhof T, Burger JA, Pritchard LK, Pugach P, Yasmeen A, et al. 2015. Immunogenicity of stabilized HIV-1 envelope trimers with reduced exposure of non-neutralizing epitopes. Cell 163:1702–1715. https://doi.org/10.1016/j.cell.2015.11.056
78. Chuang G-Y, Geng H, Pancera M, Xu K, Cheng C, Acharya P, Chambers M, Druz A, Tsybovsky Y, Wanninger TG, Yang Y, Doria-Rose NA, Georgiev IS, Gorman J, Joyce MG, O'Dell S, Zhou T, McDermott AB, Mascola JR, Kwong PD. 2017. Structure-based design of a soluble prefusion-closed HIV-1 Env trimer with reduced CD4 affinity and improved immunogenicity. J Virol 91:e02268-16. https://doi.org/10.1128/JVI.02268-16
79. Nguyen HT, Wang Q, Anang S, Sodroski JG. 2023. Characterization of the human immunodeficiency virus (HIV-1) envelope glycoprotein conformational States on infectious virus particles. J Virol 97:e0185722. https://doi.org/10.1128/jvi.01857-22
80. Zhang Z, Wang Q, Nguyen HT, Chen H-C, Chiu T-J, Smith III AB, Sodroski JG. 2023. Alterations in gp120 glycans or the gp41 fusion peptide-proximal region modulate the stability of the human immunodeficiency

virus (HIV-1) envelope glycoprotein pretriggered conformation. J Virol 97:e0059223. https://doi.org/10.1128/jvi.00592-23
81. Julien JP, Cupo A, Sok D, Stanfield RL, Lyumkis D, Deller MC, Klasse PJ, Burton DR, Sanders RW, Moore JP, Ward AB, Wilson IA. 2013. Crystal structure of a soluble cleaved HIV-1 envelope trimer. Science 342:1477–1483. https://doi.org/10.1126/science.1245625
82. Lyumkis D, Julien J-P, de Val N, Cupo A, Potter CS, Klasse P-J, Burton DR, Sanders RW, Moore JP, Carragher B, Wilson IA, Ward AB. 2013. Cryo-EM structure of a fully glycosylated soluble cleaved HIV-1 envelope trimer. Science 342:1484–1490. https://doi.org/10.1126/science.1245627
83. Pancera M, Zhou T, Druz A, Georgiev IS, Soto C, Gorman J, Huang J, Acharya P, Chuang G-Y, Ofek G, et al. 2014. Structure and immune recognition of trimeric pre-fusion HIV-1 Env. Nature 514:455–461. https://doi.org/10.1038/nature13808
84. Zhang P, Kwon AL, Guzzo C, Liu Q, Schmeisser H, Miao H, Lin Y, Cimbro R, Huang J, Connors M, Schmidt SD, Dolan MA, Armstrong AA, Lusso P, Alter G, Karim SA. 2021. Functional anatomy of the trimer apex reveals key hydrophobic constraints that maintain the HIV-1 envelope spike in a closed state. mBio 12:e00090-21. https://doi.org/10.1128/mBio.00090-21
85. Kwon YD, Pancera M, Acharya P, Georgiev IS, Crooks ET, Gorman J, Joyce MG, Guttman M, Ma X, Narpala S, et al. 2015. Crystal structure, conformational fixation and entry-related interactions of mature ligand-free HIV-1 Env. Nat Struct Mol Biol 22:522–531.
86. Hwang SS, Boyle TJ, Lyerly HK, Cullen BR. 1992. Identification of envelope V3 loop as the major determinant of CD4 neutralization sensitivity of HIV-1. Science 257:535–537. https://doi.org/10.1126/science.1636088
87. Zou S, Zhang S, Gaffney A, Ding H, Lu M, Grover JR, Farrell M, Nguyen HT, Zhao C, Anang S, Zhao M, Mohammadi M, Blanchard SC, Abrams C, Madani N, Mothes W, Kappes JC, Smith AB, Sodroski J. 2020. Long-acting BMS-378806 analogues stabilize the state-1 conformation of the human immunodeficiency virus type 1 envelope glycoproteins. J Virol 94:e00148-20. https://doi.org/10.1128/JVI.00148-20
88. Pancera M, Lai Y-T, Bylund T, Druz A, Narpala S, O'Dell S, Schön A, Bailer RT, Chuang G-Y, Geng H, Louder MK, Rawi R, Soumana DI, Finzi A, Herschhorn A, Madani N, Sodroski J, Freire E, Langley DR, Mascola JR, McDermott AB, Kwong PD. 2017. Crystal structures of trimeric HIV envelope with entry inhibitors BMS-378806 and BMS-626529. Nat Chem Biol 13:1115–1122. https://doi.org/10.1038/nchembio.2460
89. Adachi A, Gendelman HE, Koenig S, Folks T, Willey R, Rabson A, Martin MA. 1986. Production of acquired immunodeficiency syndrome-associated retrovirus in human and nonhuman cells transfected with an infectious molecular clone. J Virol 59:284–291. https://doi.org/10.1128/JVI.59.2.284-291.1986
90. Schneider CA, Rasband WS, Eliceiri KW. 2012. NIH image to imageJ: 25 years of image analysis. Nat Methods 9:671–675. https://doi.org/10.1038/nmeth.2089
91. Lowry R. 2004. Vassarstats: website for statistical computation. Available from: http://vassarstats.net/